

AD-A048 882

AIR FORCE INST OF TECH WRIGHT-PATTERSON AFB OHIO SCH--ETC F/G 15/7  
A FEASIBILITY STUDY OF A MANUAL BOMB RELEASE WHILE IN A TURN.(U)  
DEC 77 J D WALTON

UNCLASSIFIED

AFIT/OAE/AA/77D-17

NL

1 OF 2  
AD  
A048882

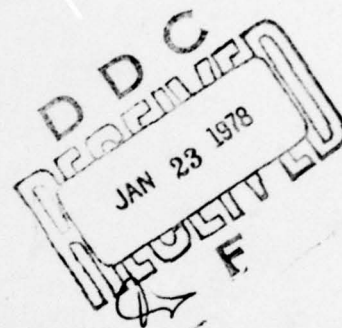


AD A U 48882

DDC FILE COPY

AFIT/GAE/AA/77D-17

P



A FEASIBILITY STUDY OF A MANUAL  
BOMB RELEASE WHILE IN A TURN

THESIS

AFIT/GAE/AA/77D-17 Joel D. Walton  
Capt USAF

Approved for public release; distribution unlimited.

(See 1473)

AFIT/GAE/AA/77D-17

A FEASIBILITY STUDY OF A MANUAL  
BOMB RELEASE WHILE IN A TURN

THESIS

Presented to the Faculty of the School of Engineering  
of the Air Force Institute of Technology  
Air University  
in Partial Fulfillment of the  
Requirements for the Degree of  
Master of Science

by

Joel D. Walton

Capt USAF

Graduate Aeronautical Engineering

December 1977

Approved for public release; distribution unlimited.

ACCESSION NO.	
NTIS	White Sect
DDC	Buff Section
ANNOUNCED	
DISTRIBUTION	
BY	
DISTRIBUTION/AVAILABILITY CODE	
or SPEC	
A	

## Preface

This thesis is an attempt to determine if a pilot is capable of manually flying an aircraft through a turning bomb run delivery. The report is limited to a frequency response analysis of the linearized system with emphasis being focused on system response due to random inputs such as turbulence. The topic for this report was suggested by Captain Bill Ashton of the Air Force Avionics Laboratory, Wright-Patterson Air Force Base, Ohio.

I wish to express my appreciation to my thesis advisor, Captain James Silverthorn for his unending assistance and invaluable advice. Without his help, I would not have been able to complete this report.

I would also like to thank Dr. Wilhelm Ericksen of the Mathematics Department and Dr. Paul Merritt of the Air Force Weapons Laboratory, Kirtland Air Force Base, New Mexico for their assistance in implementing my computer program.

Finally, I would like to thank my wife, Sandy, for her patience and understanding and her assistance in typing this report.

Joel D. Walton

Contents

	Page
Preface . . . . .	ii
List of Figures . . . . .	v
List of Tables . . . . .	vii
List of Symbols . . . . .	viii
Abstract . . . . .	xvii
I. Introduction . . . . .	1
Background . . . . .	1
Purpose . . . . .	3
Approach . . . . .	4
Limitations . . . . .	6
II. Geometry Equations . . . . .	8
III. Fire Control Bombing Law . . . . .	22
Nonlinear Fire Control Law . . . . .	22
Linear Fire Control Law . . . . .	25
IV. Turbulence Response Model . . . . .	30
V. Pilot Model . . . . .	37
Background . . . . .	37
Crossover Model . . . . .	38
System Application . . . . .	40
VI. System Evaluation and Results . . . . .	42
Form of Y . . . . .	42
Pilot Gain $G_c$ . . . . .	43
RMS Values for $\phi_c$ and $\phi$ . . . . .	44
Error Analysis . . . . .	48
Pilot Workload . . . . .	54
VII. Conclusions . . . . .	57
Bibliography . . . . .	59

Contents

	Page
Appendix A: Aircraft Characteristics . . . . .	61
Appendix B: Aircraft Equations of Motion . . . . .	64
Appendix C: Flight Control Equations . . . . .	79
Appendix D: Computer Model . . . . .	93
Vita . . . . .	103

List of Figures

<u>Figure</u>	<u>Page</u>
1 Typical Bombing Pattern . . . . .	2
2 System Model . . . . .	5
3 Relationship Between $\gamma'$ and $R_{p_0}$ . . . . .	11
4 Relationship Between $\lambda$ and $R_2$ . . . . .	12
5 Relationship Between $R_p$ and $R_L$ to the x, y, z Coordinate System . . . . .	13
6 Bank Angle $\phi$ with Respect to $\gamma^*$ . . . . .	15
7 Input PSD for Lateral and Vertical Gusts . . . . .	35
8 Input PSD for P Gusts . . . . .	36
9 Closed Loop System with Pilot Model . . . . .	40
10 System Response to a Lateral Unit Input . . . . .	43
11 Aileron Actuator . . . . .	80
12 Rudder Actuator . . . . .	80
13 Horizontal Tail Actuator . . . . .	81
14 Differential Tail Actuator . . . . .	81
15 Primary Pitch Axis Control Laws (F-15) . . . . .	85
16 Primary Roll Axis Control Laws (F-15) . . . . .	86
17 Primary Yaw Axis Control Laws (F-15) . . . . .	87
18 Augmented Pitch Axis Control Laws (Firefly) . . . . .	90
19 Augmented Roll Axis Control Laws (Firefly) . . . . .	91
20 Augmented Yaw Axis Control Laws (Firefly) . . . . .	92
21 Elements of the A Matrix . . . . .	98
22 System Model in Matrix Form for Lateral Stick Input . . . . .	101

List of Figures

<u>Figure</u>		<u>Page</u>
23	Elements of the B Matrix (F-15) . . . . .	102
24	Elements of the B Matrix (Firefly) . . . . .	102

List of Tables

<u>Table</u>	<u>Page</u>
I Summary of Geometry Equations . . . . .	20
II Summary of Nonlinear Fire Control Law . . . . .	28
III Pilot Gain . . . . .	44
IV Bank Angle Response for Aircraft without Fire Control System . . . . .	46
V Bank Angle Response for Aircraft, Fire Control System and Pilot . . . . .	47
VI Bank Angle Response where Fire Control is Connected to the Flight Controls . . . . .	48
VII Error Analysis for Aircraft without Fire Control System. (Pilot Nulls $\phi$ ) . . . . .	51
VIII Error Analysis where Pilot Nulls $\phi_c$ . . . . .	52
IX Error Analysis where Fire Control System is Connected to the Autopilot . . . . .	53
X RMS Values for Error Parameter (Level Turn) . . . . .	54
XI Summary of Linearized Aircraft Equations . . . . .	77

### List of Symbols

[A]	Matrix which depends on system components
AGL	Above ground level
$\vec{A}$	Acceleration vector which results in turn of radius $R_2$ , ft/sec <sup>2</sup>
$\vec{a}$	Total acceleration vector of the aircraft
[B]	Vector which represents the external inputs
b	Wing span, ft
$B_i$	Input matrix element
$\bar{c}$	Mean aerodynamic chord, ft
$C_x$	Force coefficient in x direction
$C_z$	Force coefficient in z direction
$C_D$	Aircraft drag coefficient
$C_L$	Aircraft lift coefficient
$C_{L_\alpha}$	Aircraft lift curve slope, rad <sup>-1</sup>
$C_y$	Force coefficient in y direction
$C_{y_\beta}$	Variation of side force coefficient with side slip angle

$C_{yp}$	Variation of side force coefficient with roll rate
$C_{yr}$	Variation of side force coefficient with yaw rate
$C_{y\delta_{DT}}$	Variation of side force coefficient with differential tail angle, $\text{rad}^{-1}$
$C_{y\delta_R}$	Variation of side force coefficient with rudder angle, $\text{rad}^{-1}$
$C_{\ell}$	Rolling moment coefficient
$C_{\ell\beta}$	Variation of rolling moment coefficient with sideslip angle
$C_{\ell p}$	Variation of rolling moment coefficient with roll rate
$C_{\ell r}$	Variation of rolling moment coefficient with yaw rate
$C_{\ell\delta_A}$	Variation of rolling moment coefficient with aileron angle, $\text{rad}^{-1}$
$C_{\ell\delta_{DT}}$	Variation of rolling moment coefficient with differential tail angle, $\text{rad}^{-1}$
$C_{\ell\delta_R}$	Variation of rolling moment coefficient with rudder angle, $\text{rad}^{-1}$
$C_m$	Aircraft pitching moment coefficient
$C_{m\alpha}$	Variation of pitching moment coefficient with angle of attack
$C_{m\dot{\alpha}}$	Variation of pitching moment coefficient with rate of change of angle of attack
$C_{mq}$	Variation of pitching moment coefficient with pitch rate

$C_{m_{\delta HT}}$	Variation of pitching moment coefficient with horizontal tail angle, $\text{rad}^{-1}$
$C_n$	Aircraft yawing moment coefficient
$C_{n_{\beta}}$	Variation in yawing moment coefficient with sideslip angle
$C_{n_p}$	Variation in yawing moment coefficient with roll rate
$C_{n_r}$	Variation in yawing moment coefficient with yaw rate
$C_{n_{\delta A}}$	Variation in yawing moment coefficient with aileron angle, $\text{rad}^{-1}$
$C_{n_{\delta DT}}$	Variation of yawing moment coefficient with differential tail angle, $\text{rad}^{-1}$
$C_{n_{\delta R}}$	Variation of yawing moment coefficient with rudder angle, $\text{rad}^{-1}$
D	Aircraft drag, lbs
$D_p$	Drag correction factor
F, f	Force (total, perturbed), lbs
$F_{AS}$	Lateral stick force, lbs
$F_{ES}$	Longitudinal stick force, lbs
$F_{RP}$	Rudder pedal force, lbs
G	Height of aim point, p, above target, ft
$g_c$	Acceleration due to gravity, $\text{ft}/\text{sec}^2$
G(s)	Transfer function

$\vec{H}$	Angular momentum vector, slug-ft <sup>2</sup> /sec
h	Height of aircraft above the target, ft
$I_x$	Moment of inertia about the x axis, slug ft <sup>2</sup>
$I_y$	Moment of inertia about the y axis, slug ft <sup>2</sup>
$I_z$	Moment of inertia about the z axis, slug ft <sup>2</sup>
$I_{xz}$	Product of inertia, slug ft <sup>2</sup>
j	$(-1)^{\frac{1}{2}}$
$K_c$	System gain
$K_p$	Pilot gain
$K_D$	Drag parameter for the bomb, ft <sup>-1</sup>
$L, \ell$	Rolling moment (total, perturbed), ft-lbs
L	Lift, lbs
$L_i$	Scaling factor for wind gusts, ft
$\vec{M}$	Applied moment, ft-lbs
M, m	Pitching moment (total, perturbed), ft-lbs
m	Mass of the aircraft, slugs
N, n	Yawing moment (total, perturbed), ft-lbs
n	Load factor

$P, p$	Roll rate (total, perturbed), rad/sec
$P_c, p_c$	Fire control roll rate command (total, perturbed), rad/sec
PSD	Power spectral density
$Q, q$	Pitch rate (total, perturbed), rad/sec
$\bar{q}$	Dynamic pressure, lbs/ft <sup>2</sup>
$[R]$	Vector representing perturbation variables
$R, r$	Yaw rate (total, perturbed), rad/sec
$R_2$	Aircraft turn radius, ft
$R_{D2}$	Denominator, fire control equation
RMS	Root-Mean-Square
$R_p$	Range from aircraft to air mass aim point, ft
$R_R$	Release range to air mass aim point, ft
$R_T$	Slant range to the target, ft
$S$	Wing surface area, ft <sup>2</sup>
$s$	Laplace transform variable
$T, t$	Thrust (total, perturbed), lbs
$[T]$	General Euler transformation matrix

$T_f, t_f$	Time of fall of the bomb (total, perturbed), sec
$T_I$	Pilot lag time constant, sec
$T_L$	Pilot lead time constant, sec
$T_N$	Pilot neuromuscular lag time constant, sec
$U, u$	Velocity along x axis (total, perturbed), ft/sec
$V, v$	Aircraft velocity along y axis (total, perturbed), ft/sec
$V_T$	True airspeed of the aircraft, ft/sec
$W, w$	Aircraft velocity along z axis (total, perturbed)
$X$	Longitudinal axis of the aircraft (body fixed)
$Y_c$	Controlled element describing function
$Y$	Lateral axis of the aircraft (body fixed)
$Y_{OL}$	Open loop describing function - $Y_p Y_c$
$Y_p$	Pilot describing function
$Z$	Vertical axis of the aircraft (body fixed, positive downward)
$\bar{\alpha}, \alpha$	Angle of attack (total, perturbed), rad
$\alpha_o$	Trim angle of attack, rad
$\beta$	Sideslip angle (perturbed), rad

$\bar{\gamma}$	Angle between $R_T$ and the horizontal, rad
$\gamma'$	Angle between $R_T$ and $R_p$ , rad
$\gamma''$	Flight path angle, rad
$\gamma^*$	Angle between $\bar{A}$ and the horizontal, rad
$\delta_A$	Aileron deflection angle, rad
$\delta_{DT}$	Differential tail deflection angle, rad
$\delta_{HT}$	Horizontal tail deflection angle, rad
$\delta_R$	Rudder deflection angle, rad
$\bar{\lambda}, \lambda$	Angle between $V_T$ and $R_p$ (total, perturbed), rad
$\rho$	Air density, slugs/ft <sup>3</sup>
$\rho/\rho_0$	Air density ratio
$\phi, \phi$	Roll angle (total, perturbed), rad
$[\phi]$	Roll transformation matrix
$\phi$	Phase angle, rad or deg
$\phi_c$	Command bank angle, rad
$\phi_{i_g}$	Power spectral density due to wind gust in the $i$ th direction
$\theta, \theta$	Pitch attitude angle (total, perturbed), rad
$[\theta]$	Pitch transformation matrix

$\Psi, \psi$	Horizontal Euler Angle between the nose of the Aircraft and $R_{p_0}$ (total, perturbed), rad
$[\psi]$	Yaw transformation matrix
$\Omega_w, \omega_w$	Angular velocity about the body fixed z axis (total, perturbed), rad/sec
$\vec{\omega}$	Angular velocity of the aircraft, rad/sec
$\omega$	Frequency, hertz, rad/sec
$\omega_c$	Cut off frequency, hertz, rad/sec
$\omega_i$	Input frequency, hertz, rad/sec
$\tau$	Pilot's transport time delay, sec
$\tau_e$	Pilot's effective time delay, sec
$\sigma_e$	RMS miss distance (total), ft
$\sigma_i$	Root mean square gust intensity in the ith direction, ft/sec
$\sigma_{\phi_c}$	RMS value for perturbed command bank angle, deg
$\sigma_{\phi}$	RMS value for perturbed bank angle, deg
$\frac{d}{dt}$	Differentiation with respect to time
$   $	Magnitude
$[ ]$	Matrix

Subscripts

A	Aerodynamic
T	Thrust
o	Steady state
g	Gust
x, y, z	Components along x, y, z axis respectively
elec	Electrical input
mech	Mechanical input

Super scripts

→	Vector
-	Total angle
T	Transpose

Abstract

This study attempts to determine if a pilot can manually release a bomb while in a turn. The nonlinear equations describing the geometry, fire control law, aircraft equations of motion, flight controls and pilot model are developed. These equations are linearized so that a frequency response analysis can be conducted for perturbations about a nominal trajectory. The system response is evaluated using wind gust inputs and lateral stick inputs and plotting the resulting system perturbations over a given frequency range. The results of this analysis indicate the pilot is capable of manually releasing a bomb while in a turn. His performance which is determined by the magnitude of the resulting perturbations is comparable to the fully automated system. This roll task does not create an excessive workload for the pilot.

## I. Introduction

### Background

During recent years there has been a growing need for a change in bomb delivery tactics. This is primarily due to enemy defenses being equipped with radar guided weapons. For example, the new Russian anti-aircraft guns, which use linear predictors as part of their aiming systems, are believed to be extremely accurate when used against aircraft in a wings level, low "g" maneuver. Therefore, in a heavily defended environment, it is desirable that an aircraft be continually making heading and altitude changes to complicate the enemies tracking problems.

Current bombing tactics and equipment require an aircraft to track the target. This is a wings level, relatively low "g" maneuver which requires several seconds for an accurate release. This maneuver falls well within the enemies capabilities for tracking and predicting the flight path of the aircraft and greatly increases the chances of the aircraft being destroyed. This gives rise to the need for a new approach to get the aircraft to a reliable release point.

This new approach is currently being studied by the Air Force through a contract with the General Electric Company. A fire control system (FCS) is being developed by GE under the project name "Firefly". This FCS has the capability of tracking a target, computing a release point, and directing the autopilot to fly the aircraft to this release point (Fig. 1). The flight path from the point where the system is engaged to the bomb release point is primarily determined by the number of "g's" which the pilot wishes to use. When

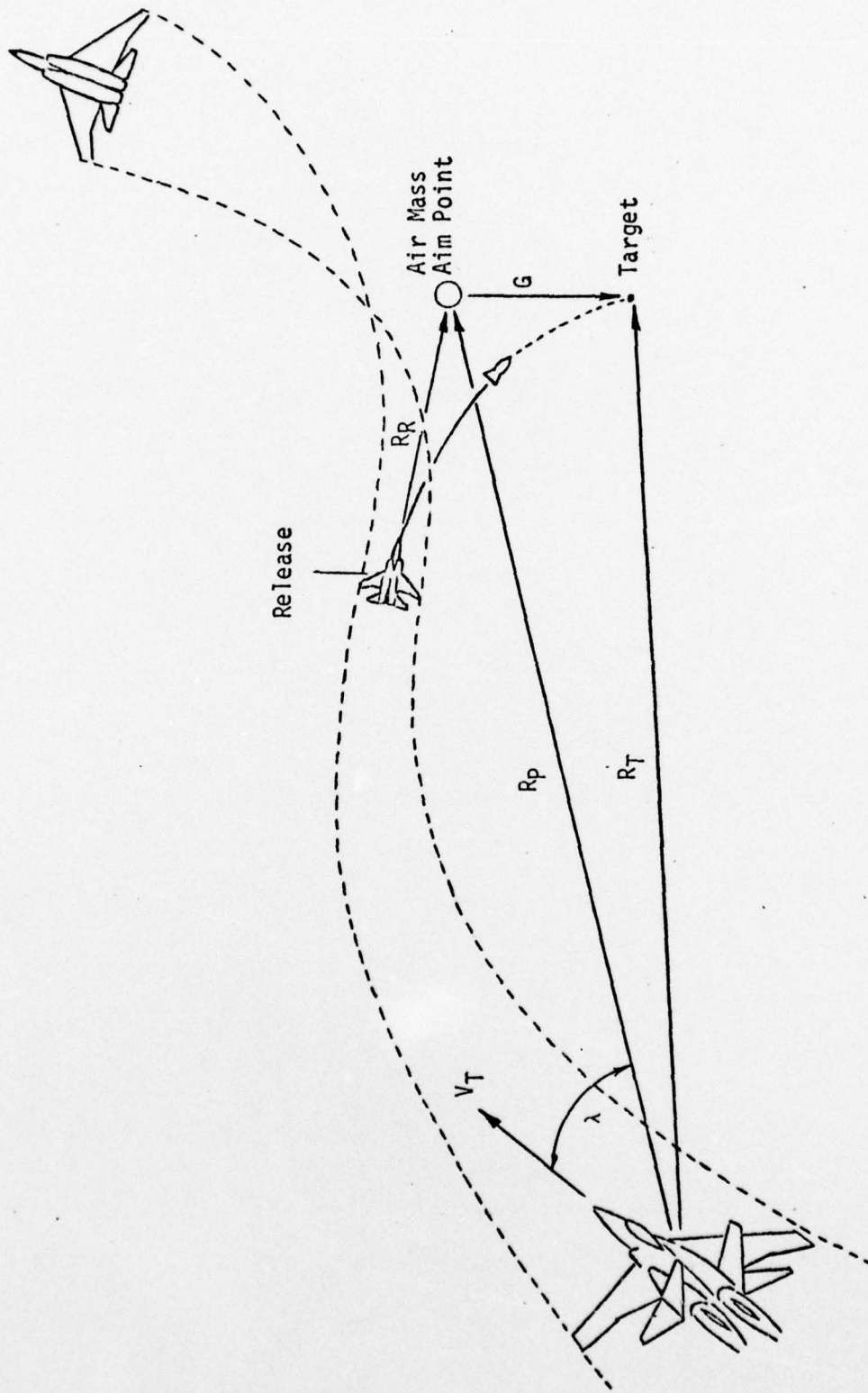


Fig. 1. Typical Bombing Pattern

the FCS is engaged, the system maintains this same load factor and computes the required bank angle to take the aircraft to the computed release point. If the aircraft is fairly close to the target for a given load factor, the bank angle will be relatively steep to accommodate a diving turn and hence, a short release range. However, if the distance to the target is much greater for the same number of "g's", the bank angle will be shallow to allow a climbing trajectory which results in a greater release range. The only restrictions on the system are:

- (1) For a particular load factor, the aircraft must be close enough to the target, so that the bomb can be "tossed" into the target through a lofted trajectory.
- (2) For a close in position, the roll attitude is restricted so as to ensure ground clearance (Ref 1:5.1-5.3).

#### Purpose

The purpose of this study is to determine if a pilot can manually fly the aircraft through basically the same maneuver that would be accomplished by the FCS coupled to the flight control system. For this analysis, the same target information will be delivered to the FCS, however, the output from the fire control will go to a heads-up-display (HUD) instead of the flight controls. It will then be the pilot's task to determine an acceptable load factor and to trim the aircraft accordingly. He will then be required to follow the roll commands as displayed on the HUD.

If this approach proves feasible, then the flight control coupler can be disconnected from the FCS so the pilot is in full control of the aircraft throughout this very critical maneuver when evasive action may be required at any time. This will not only result in a more responsive

aircraft for evasive maneuvers but will eliminate the need for the equipment which will tie the FCS into the flight controls.

#### Approach

This study is based upon the system model shown in figure 2 where the pilot is attempting to null the error signal displayed on the HUD. The error signal is a result of the external inputs such as wind gusts disturbing the aircraft motion from some equilibrium or nominal trajectory. As a result of these disturbances, perturbation signals are fed back into the flight controls by the stability augmentation and control augmentation systems. These disturbances in the flight controls along with the pilot lateral stick inputs produce control surface deflections which in turn affects the aircraft motion. The fire control law then determines a roll rate command based upon the aircraft motion and the position and orientation of the aircraft relative to the target. The roll rate command is then integrated to obtain a bank angle command which is displayed on the HUD.

In order to analyze this system, it is first necessary to obtain the nonlinear differential and algebraic equations which represent the following subsystems:

- (1) Aircraft
- (2) Flight controls
- (3) Geometry (Aircraft position relative to the target)
- (4) Fire control
- (5) Turbulance model
- (6) Pilot model

The geometry equations provide the nominal conditions required to define the trajectory which will take the aircraft to an accurate release point. Since the nominal conditions are defined as an equilibrium condition, it

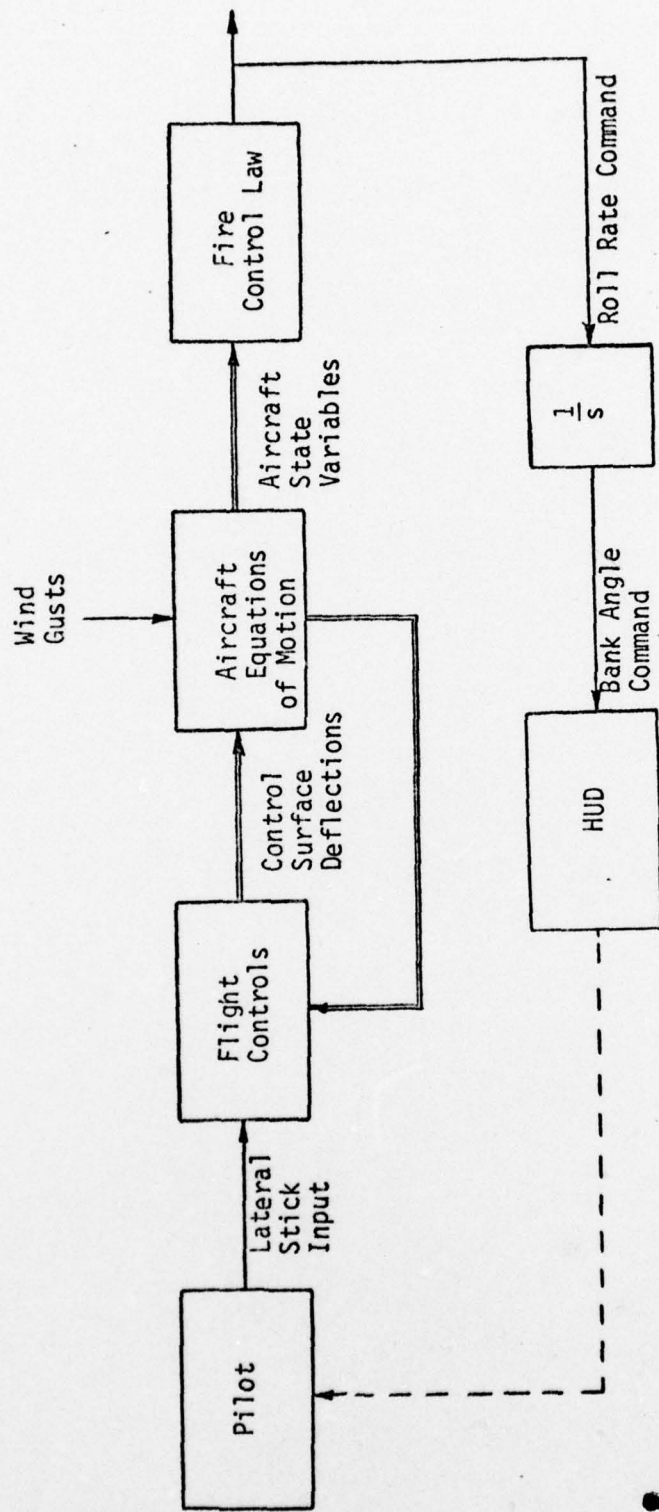


Fig. 2. System Model

is appropriate to use the small perturbation technique to study the system response. Since frequency response is useful in analyzing the system response, the nonlinear equations have been linearized by using the Taylor's series expansion and retaining only the linear terms. The computer program described in Appendix D solves these linear equations by evaluating the wind gust inputs or lateral stick inputs and plotting the resulting perturbations over a given frequency range.

Knowing the lateral response of the system and the magnitude of the perturbations involved, it is possible to compare how well the manual system responds to the fully automated system. Also, knowing the magnitude of the perturbations makes it possible to determine how large a miss distance one might expect due to disturbances such as wind gusts. Finally, a Cooper-Harper rating can be determined which is indicative of the pilot's workload for this roll task.

#### Limitations

This study is restricted to classical frequency response analysis. Therefore, the final equations are linear and time invariant. Inputs to the system are restricted to lateral stick movements and turbulence. Since the F-15 aircraft flight controls are designed to maintain coordinated flight without the aid of the pilot, rudder inputs are not considered. Also, longitudinal stick inputs as a result of lateral stick movement have not been considered for the following two reasons:

1. The aircraft is in a trimmed maneuver requiring no back stick pressure to maintain the desired load factor.
2. Precision control of the aircraft load factor is not a requirement for this system (Ref 1:5.1).

The effects due to equipment noise or measurement errors are not discussed

in this report.

In order to simplify the equations of motion, a constant speed of 0.6 Mach has been used as the nominal velocity. For a density altitude of  $\rho/\rho_0$  equal to 0.971 (which has also been assumed to be a constant), the total steady state velocity of the aircraft is 665 feet per second. A constant density altitude has been assumed since it is envisioned that the majority of the weapon delivery modes will have less than a 15 degree flight path angle for the European theater where low overcast skies will restrict the height of the aircraft above the target. For this same reason, the aircraft trajectories modelled in this report are either level or shallow descending turns.

## II. Geometry Equations

The linear fire control bombing law, which is developed in Chapter 3, is designed to null the perturbations about a nominal trajectory. To accomplish this, it is first necessary to determine the nominal parameters which define this trajectory. The approach used in this study assumes the initial conditions are the nominal values which will result in an accurate solution. That is, if no disturbances or inputs are added to the system, the orientation of the aircraft is such that it will fly to an accurate release point. This approach, in effect, freezes the aircraft at different points along the flight path so that the response of the system may be analyzed at these various conditions. The equations which are developed in this chapter determine the nominal conditions for the angle of attack, the Euler angles and the different ranges involved.

First, in order to obtain these nominal values, it has been assumed that the position of the aircraft relative to the target is known. This is not an unreasonable assumption since onboard equipment is capable of providing this information. The following three parameters fix the aircraft position relative to the target:

- $R_{T_0}$  - The slant range from the aircraft to the target
- $h$  - Height of the aircraft above the target
- $\lambda_0$  - Angle between the velocity vector of the aircraft and the vector from the aircraft to the air mass aim point, a distance  $G_0$  above the target.

Knowing these three quantities plus the velocity of the aircraft and

the desired time of fall of the bomb, the necessary nominal values for the fire control law can be determined. These nominal values are:

1.  $G_o$  - Height of the aim point above the target.
2.  $R_{R_o}$  - Distance from the release point to the aiming point.
3.  $\gamma_o$  - The angle between  $R_{T_o}$  and the horizontal.
4.  $R_{P_o}$  - Range from the aircraft to the aiming point.
5.  $\alpha_o$  - Angle of attack.
6.  $\psi_o, \theta_o, \phi_o$  - Euler angles for yaw, pitch and roll.

Although the nominal time of fall is not a fixed parameter in the actual "Firefly" control system, it has been given a fixed value here to simplify the calculations. Where an infinite number of solutions existed before, now only one solution exists.

The aimpoint P is defined as being a gravity drop distance  $G_o$  directly above the target which is given approximately by:

$$G_o = .5 D_p g_c T_{f_o}^2 \quad (2-1)$$

$$\text{where } D_p = 1 - K_D (\rho/\rho_o) V_{T_o} T_{f_o} \quad (2-2)$$

$K_D$  = Drag constant of the bomb

$$= 2.4 (10^{-6}) \text{ ft}^{-1} \text{ for low drag MK83}$$

$\rho/\rho_o$  = Relative air density

$$= .971 \text{ for this analysis}$$

$T_{f_o}$  = Time of fall of the weapon

$V_{T_o}$  = Inertial velocity of the aircraft

$$= 665 \text{ ft/sec}$$

$g_c =$  Gravitational constant

$$= 32.2 \text{ ft/sec}^2 \quad (\text{Ref 2:14})$$

The release range, which is defined as the distance from the point of release of the bomb to the aim point P, is given by:

$$R_R = D_p V_{T_o} T_{f_o} \quad (2-3)$$

(Ref 2:15)

Note that the angle between the horizontal and  $R_{T_o}$  is defined as positive downward as shown in Fig. 3. The value for this angle is given by:

$$\gamma_o = \sin^{-1}(h/R_{T_o}) \quad (2-4)$$

The angle  $\gamma'$  is also defined as positive downward as shown in Fig. 3.

From Fig. 3, the following relationship may be realized:

$$G_o = \frac{R_{T_o} \sin \gamma'}{\cos(\gamma_o - \gamma')} \quad (2-5)$$

It follows that,

$$\tan \gamma' = \frac{G_o \cos \gamma_o}{R_{T_o} - G_o \sin \gamma_o} \quad (2-6)$$

From Fig. 3,  $R_{p_o}$  can be determined using the law of cosines and the quadratic equation:

$$G_o^2 = R_{p_o}^2 + R_{T_o}^2 - 2 R_{T_o} R_{p_o} \cos \gamma' \quad (2-7)$$

or,

$$R_{p_o} = R_{T_o} \cos \gamma' - (G_o^2 - R_{T_o}^2 \sin^2 \gamma')^{1/2} \quad (2-8)$$



result in a greater time of fall to account for the air mass aimpoint being higher. This in turn raises the vector  $\vec{R}_{P_0}$  to coincide with the new plane in which the velocity vector now rests. In this way, the actual fire control system is able to update itself so as to provide a continuous solution as the aircraft maneuvers.

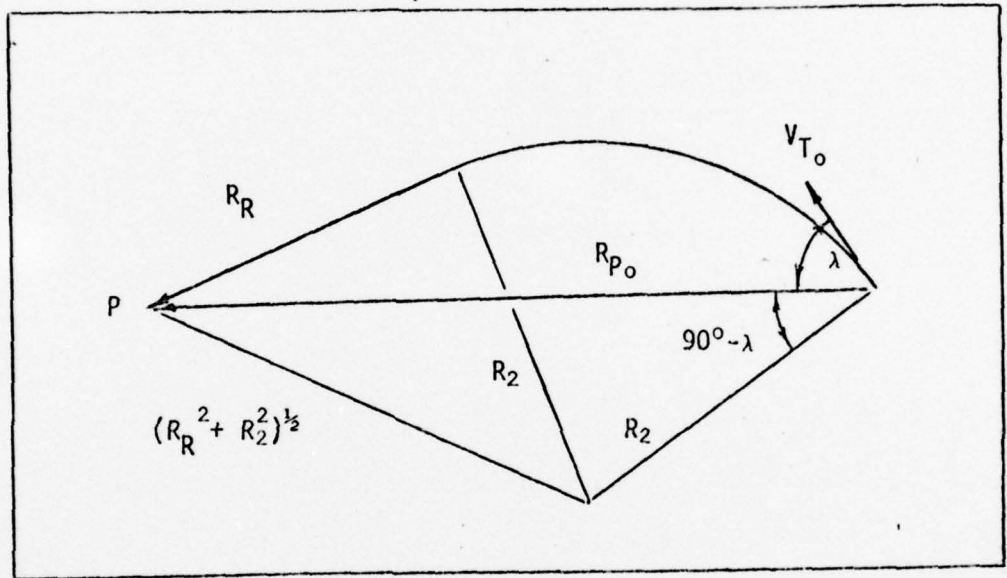


Fig. 4. Relationship Between  $\lambda$  and  $R_2$

From Fig. 4, and using the law of cosines,  $R_2$ , the radius of turn can be defined as:

$$R_2 = \frac{R_{P_0}^2 - R_{R_0}^2}{2R_{P_0} \sin \lambda_0} \quad (2-9)$$

Note that the angle  $\lambda_0$  is defined as positive for a clockwise direction and is negative as shown in Fig. 4. Due to the effect of the sign on different angles, all equations in this section are defined for an aircraft attacking the target from an orbit which is counter clockwise with

respect to the target.

To determine the bank angle required to maintain the aircraft in the desired plane with a radius of turn equal to  $R_2$ , it is first necessary to determine the direction of the force in the plane which produces the turn. To do this, one must first define an equation for this plane. Knowing that  $\vec{R}_{P_0}$  and  $\vec{R}_L$  both lie in this plane and are perpendicular to each other, the unit vector  $\hat{n}$ , which is perpendicular to the plane can be developed as follows:

$$\hat{n} = \frac{\vec{R}_{P_0} \times \vec{R}_L}{|\vec{R}_{P_0} \times \vec{R}_L|} \quad (2-10)$$

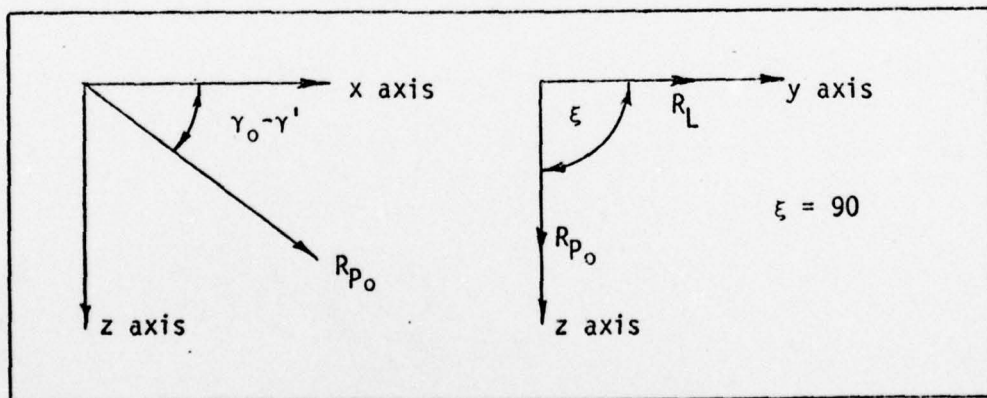


Fig. 5. Relationship Between  $R_{P_0}$  and  $R_L$  to the  $x, y, z$  Coordinate System

From Fig. 5:

$$\vec{R}_{P_0} = \begin{bmatrix} R_{P_0} \cos (\gamma_0 - \gamma') \\ 0 \\ R_{P_0} \sin (\gamma_0 - \gamma') \end{bmatrix}$$

$$\vec{R}_L = \begin{bmatrix} 0 \\ R_L \\ 0 \end{bmatrix}$$

$$\hat{n} = -\sin (\gamma_0 - \gamma') \hat{i} + \cos (\gamma_0 - \gamma') \hat{k} \quad (2-11)$$

Let the force in the plane which produces the turn be defined as:

$$\vec{F} = m\vec{A} = m (A_x \hat{i} + A_y \hat{j} + A_z \hat{k}) \quad (2-12)$$

Since  $\vec{A}$  and  $\hat{n}$  are perpendicular:

$$\vec{A} \cdot \hat{n} = -A_x \sin (\gamma_0 - \gamma') + A_z \cos (\gamma_0 - \gamma') = 0 \quad (2-13)$$

$$A_z = A_x \frac{\sin (\gamma_0 - \gamma')}{\cos (\gamma_0 - \gamma')} \quad (2-14)$$

also:  $\vec{A} \cdot \vec{R}_{P_0} = A R_{P_0} \cos (90^\circ - \lambda_0)$

$$= A_x R_{P_x} = A_z R_{P_z} \quad (2-15)$$

$$A_x = A \cos (\gamma_0 - \gamma') \sin \lambda_0 \quad (2-16)$$

Therefore:

$$A_z = A \sin (\gamma_0 - \gamma') \sin \lambda_0 \quad (2-17)$$

The angle between the horizontal and the vector  $\vec{A}$  is then given by:

$$\sin \gamma^* = \frac{A_z}{A}$$

$$\sin \gamma^* = \sin (\gamma_o - \gamma') \sin \lambda_o \quad (2-18)$$

It should be noted that  $\gamma^*$  is positive downward. Knowing  $\gamma^*$  and recalling that  $A$  can be set equal to  $\frac{V_{T_o}^2}{R_2}$ , the bank angle  $\phi_o$  can now be determined with the aid of Fig. 6.

$$\tan \phi_o = \frac{\frac{V_{T_o}^2}{R_2} \cos \gamma^*}{g_c - \frac{V_{T_o}^2 \sin \gamma^*}{R_2}} \quad (2-19)$$

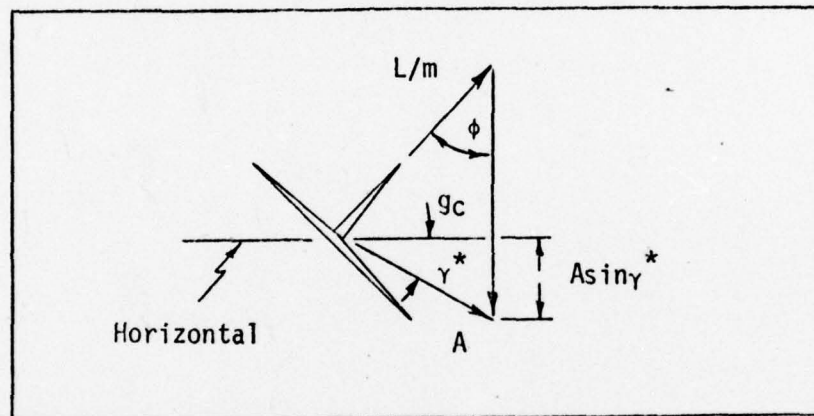


Fig. 6. Bank Angle  $\phi$  with Respect to  $\gamma^*$

Figure 6 may also be used to determine the wing loading where:

$$\cos \phi_o = \frac{g_c - A \sin \gamma^*}{L/m} \quad (2-20)$$

$$n = \frac{L/m}{g_c} = \frac{g_c - A \sin \gamma^*}{g_c \cos \phi_o} \quad (2-21)$$

where  $n$  is the load factor.

For straight and level flight where  $n$  is equal to one, the angle of

attack may be determined as follows:

$$mg_c = \frac{1}{2} \rho V_{T_o}^2 S C_L \quad (2-22)$$

where

$$\alpha_o = \frac{C_L}{C_{L\alpha}}$$

$$= \frac{2 mg_c}{\rho V_{T_o}^2 S C_{L\alpha}}$$

$$= .02974 \text{ radians for } n = 1^\dagger$$

For any given flight condition, the angle of attack is given by:

$$\alpha_o = .02974 n$$

$$= .02974 \frac{g_c - \frac{V_{T_o} \sin \gamma^*}{R_2}}{g_c \cos \phi_o} \quad (2-23)$$

In order to determine the Euler angle  $\theta_o$ , it is necessary to find the flight path angle  $\gamma$ ". Let the velocity vector of the aircraft be defined as:

$$\vec{V}_{T_o} = U_o \hat{i} + V_o \hat{j} + W_o \hat{k} \quad (2-24)$$

Since the velocity vector is perpendicular to  $\hat{n}$ , the dot product may be written as:

$$\vec{V}_{T_o} \cdot \hat{n} = -U_o \sin(\gamma_o - \gamma') + W_o \cos(\gamma_o - \gamma') = 0 \quad (2-25)$$

$$W_o = U_o \tan(\gamma_o - \gamma') \quad (2-26)$$

The dot product for the velocity vector and the position vector yields:

$$\vec{V}_{T_o} \cdot \vec{R}_{p_o} = V_{T_o} R_{p_o} \cos \lambda_o \quad (2-27)$$

<sup>†</sup>For flight conditions given in Appendix A.

where  $R_{p_0}$  is defined in Fig. 5.

$$V_{T_0} R_{p_0} \cos \lambda_0 = U_0 R_{p_0} \cos (\gamma_0 - \gamma') + W_0 R_{p_0} \sin (\gamma_0 - \gamma') \quad (2-28)$$

Substituting equation (2-26) for  $W_0$ , the longitudinal velocity is:

$$U_0 = V_{T_0} \cos (\gamma_0 - \gamma') \cos \lambda_0 \quad (2-29)$$

It then follows that:

$$W_0 = V_{T_0} \sin (\gamma_0 - \gamma') \cos \lambda_0 \quad (2-30)$$

The flight path angle can now be determined by:

$$\sin \gamma'' = \frac{W_0}{V_{T_0}} = \sin (\gamma_0 - \gamma') \cos \lambda_0 \quad (2-31)$$

$$\text{also, } V_{T_0}^2 = U_0^2 + V_0^2 + W_0^2 \quad (2-32)$$

$$\begin{aligned} V_0 &= \left[ V_{T_0}^2 - V_{T_0}^2 \cos^2 (\gamma_0 - \gamma') \cos^2 \lambda_0 - V_{T_0}^2 \sin^2 (\gamma_0 - \gamma') \cos^2 \lambda_0 \right]^{1/2} \\ &= V_{T_0} (1 - \cos^2 \lambda_0)^{1/2} \\ &= V_{T_0} \sin \lambda_0 \end{aligned} \quad (2-33)$$

To describe vectors in the aircraft reference frame, it is helpful to use the Euler transformation matrices as follows:

$$\begin{bmatrix} \hat{x} \\ \hat{y} \\ \hat{z} \end{bmatrix} = [T] \begin{bmatrix} \hat{i} \\ \hat{j} \\ \hat{k} \end{bmatrix} = [\phi][\theta][\psi] \begin{bmatrix} \hat{i} \\ \hat{j} \\ \hat{k} \end{bmatrix} \quad (2-34)$$

Where  $\hat{x}$ ,  $\hat{y}$  and  $\hat{z}$  describe the body fixed aircraft coordinate system and  $\hat{i}$ ,  $\hat{j}$  and  $\hat{k}$  relate to the earth fixed coordinate system.

$$\begin{aligned}
[T] &= \begin{bmatrix} 1 & 0 & 0 \\ 0 & \cos\phi_0 & \sin\phi_0 \\ 0 & -\sin\phi_0 & \cos\phi_0 \end{bmatrix} \begin{bmatrix} \cos\theta_0 & 0 & -\sin\theta_0 \\ 0 & 1 & 0 \\ \sin\theta_0 & 0 & \cos\theta_0 \end{bmatrix} \begin{bmatrix} \cos\psi_0 & \sin\psi_0 & 0 \\ -\sin\psi_0 & \cos\psi_0 & 0 \\ 0 & 0 & 1 \end{bmatrix} \\
&= \begin{bmatrix} \cos\psi_0 \cos\theta_0 & \sin\psi_0 \cos\theta_0 & -\sin\theta_0 \\ \cos\psi_0 \sin\theta_0 \sin\phi_0 - \sin\psi_0 \cos\phi_0 & \sin\psi_0 \sin\theta_0 \sin\phi_0 + \cos\psi_0 \cos\phi_0 & \cos\theta_0 \sin\phi_0 \\ \cos\psi_0 \sin\theta_0 \cos\phi_0 + \sin\psi_0 \sin\phi_0 & \sin\psi_0 \sin\theta_0 \cos\phi_0 - \cos\psi_0 \sin\phi_0 & \cos\theta_0 \cos\phi_0 \end{bmatrix}
\end{aligned}$$

The aircraft velocity may then be expressed as:

$$\begin{bmatrix} U_0 \\ V_0 \\ W_0 \end{bmatrix} = \begin{bmatrix} V_{T_0} \cos\alpha_0 \\ 0 \\ V_{T_0} \sin\alpha_0 \end{bmatrix} = [T] \begin{bmatrix} V_{T_0} \cos(\gamma_0 - \gamma') \\ 0 \\ V_{T_0} \sin(\gamma_0 - \gamma') \end{bmatrix} \quad (2-35)$$

where  $V_{T_0}$  is aligned with  $R_{p_0}$ .

For level flight,  $\gamma'' = \gamma_0 - \gamma' = 0$ , the above velocity equations then reduce to:

$$\cos\alpha_0 = \cos\psi_0 \cos\theta_0 \quad (2-36)$$

$$0 = \cos\psi_0 \sin\theta_0 \sin\phi_0 - \sin\psi_0 \cos\phi_0 \quad (2-37)$$

$$\sin\alpha_0 = \cos\psi_0 \sin\theta_0 \cos\phi_0 + \sin\psi_0 \sin\phi_0 \quad (2-38)$$

The angles  $\psi_0$  and  $\theta_0$  are unknown in the above equations. The functions containing  $\psi_0$  may be replaced by functions containing  $\alpha_0$ ,  $\theta_0$ , and  $\phi_0$ .

It is then possible to solve for  $\theta_0$  as:

$$\tan\theta_0 = \tan\alpha_0 \cos\phi_0 \quad (2-39)$$

For a climbing or descending turn,

$$\tan(\theta_0 + \gamma'') = \tan\alpha_0 \cos\phi_0 \quad (2-40)$$

$$\tan \theta_o = \frac{\tan \alpha_o \cos \phi_o - \tan \gamma''}{1 + \tan \alpha_o \cos \phi_o \tan \gamma''} \quad (2-41)$$

The last remaining unknown is the Euler angle  $\psi_o$ . Using the Euler transformation matrix and the more general case where  $V_{T_o}$  is not aligned with  $R_{p_o}$ , the aircraft velocities may be expressed as:

$$\begin{bmatrix} V_{T_o} \cos \alpha \\ 0 \\ V_{T_o} \sin \alpha_o \end{bmatrix} = [T] \begin{bmatrix} V_{T_o} \cos(\gamma_o - \gamma') \cos \lambda_o \\ V_{T_o} \sin \lambda_o \\ V_{T_o} \sin(\gamma_o - \gamma') \cos \lambda_o \end{bmatrix} \quad (2-42)$$

Where the velocities for the earth fixed coordinate system come from equations (2-29), (2-30) and (2-33). The only unknown in this expression is  $\psi_o$  which may be written as:

$$\cos \psi_o = \left[ \cos \alpha_o \cos(\gamma_o - \gamma') \cos \lambda_o \cos \theta_o + \cos \phi_o \sin \alpha_o \cos(\gamma_o - \gamma') \cos \lambda_o \sin \theta_o - \sin \phi_o \sin \alpha_o \sin \lambda_o \right] / \left[ \cos^2(\gamma_o - \gamma') \cos^2 \lambda_o + \sin^2 \lambda_o \right] \quad (2-43)$$

Table I presents a summary of the geometry equations defining the steady state input parameters used in the fire control equation.

Table I

Summary of Geometry Equations

Fixed  
Parameters

$$V_{T_o} \longrightarrow D_p = 1 - K_D \rho/\rho_o V_{T_o} T_{f_o}$$

$$G_o = .5 D_p g_c T_{f_o}^2$$

$$T_{f_o} \longrightarrow R_{R_o} = D_p V_{T_o} T_{f_o}$$

$$R_{T_o} \longrightarrow \gamma_o = \sin^{-1} \left( \frac{h}{R_{T_o}} \right)$$

$$h \longrightarrow \gamma' = \tan^{-1} \left( \frac{G_o \cos \gamma_o}{R_{T_o} - G_o \sin \gamma_o} \right)$$

$$\lambda_o \longrightarrow R_{P_o} = R_{T_o} \cos \gamma' - (G_o^2 - R_{T_o}^2 \sin^2 \gamma')^{1/2}$$

$$g_c \longrightarrow R_2 = \frac{R_{P_o}^2 - R_{R_o}^2}{2 R_{P_o} \sin \lambda_o}$$

$$\gamma^* = \sin^{-1} [\sin(\gamma_o - \gamma') \sin \lambda_o]$$

$$\rho/\rho_o \longrightarrow \phi_o = \tan^{-1} \left[ \frac{\frac{V_{T_o}^2 \cos \gamma^*}{R_2}}{g_c - \frac{V_{T_o}^2 \sin \gamma^*}{R_2}} \right]$$

$$K_D \longrightarrow \alpha_o = \left( \frac{V_{T_o}^2}{g_c - R_2 \sin \gamma^*} \right) (.02974)$$

Table I (Continued)

Summary of Geometry Equations

Fixed  
Parameters

$V_{T_0}$

$$\gamma'' = \sin^{-1} [\sin(\gamma_0 - \gamma') \cos \lambda_0]$$

$T_{f_0}$

$$\theta_0 = \tan^{-1} \left[ \frac{\tan \alpha_0 \cos \phi_0 - \tan \gamma''}{1 + \tan \alpha_0 \cos \phi_0 \tan \gamma''} \right]$$

$R_{T_0}$

$$\psi_0 = \cos^{-1} \left[ \cos \alpha_0 \cos(\gamma_0 - \gamma') \cos \lambda_0 \cos \theta_0 + \cos \phi_0 \sin \alpha_0 \cos(\gamma_0 - \gamma') \cos \lambda_0 \sin \theta_0 - \right.$$

$h$

$$\left. \sin \phi_0 \sin \alpha_0 \sin \lambda_0 \right] \frac{1}{\cos^2(\gamma_0 - \gamma') \cos^2 \lambda_0 + \sin^2 \lambda_0}$$

$\lambda_0$

$g_c$

$\rho/\rho_0$

$K_D$

### III. Fire Control Law

As mentioned in the introduction, the fire control bombing law controls the bank angle of the aircraft in order to achieve a solution. It is able to accomplish this by maintaining a constant load factor while varying the bank angle which raises or lowers the velocity vector. When the velocity vector passes above the target, it should be at the correct inclination so that the bomb will cover the horizontal distance to the target during the time it takes the bomb to fall to the target. For the purposes of this study, the fire control law can be broken down into two segments, the steady state condition portion which represents the nominal solution and the perturbed condition which represents the errors due to external disturbances.

#### Nonlinear Fire Control Law

It is first necessary to express the fire control bombing law in terms of the geometry parameters developed in chapter two. The nominal flight path of the aircraft has been determined by fixing: the position of the aircraft relative to the target, the height of the air mass aimpoint above the target, and the velocity of the aircraft. With the geometry thus defined, it is now possible to write the nonlinear fire control law in terms of:

1. The state variables:  $\bar{\alpha}$ ,  $\psi$ ,  $\theta$ ,  $\phi$ .
2. The position vectors:  $G$ ,  $R_p$ ,  $R_R$ ,  $R_T$ ,  $h$
3. The parameters:  $T_f$ ,  $\bar{y}$ ,  $V_T$ ,  $\bar{x}$

where  $G = .5 \left[ 1 - K_D (\rho/\rho_o) V_T T_f \right] g_c T_f^2$  (3-1)

$$R_R = \left[ 1 - K_D (\rho/\rho_o) V_T T_f \right] V_T T_f \quad (3-2)$$

$$\bar{\gamma} = \sin^{-1} \left( \frac{h}{R_T} \right) \quad (3-3)$$

$$R_P = R_T \cos \left[ \tan^{-1} \left( \frac{G \cos \gamma}{R_T - G \sin \gamma} \right) \right] - \left\{ G^2 - \right. \quad (3-4)$$

$$\left. R_T^2 \sin^2 \left[ \tan^{-1} \left( \frac{G \cos \gamma}{R_T - G \sin \gamma} \right) \right] \right\}^{\frac{1}{2}}$$

Since  $G$ ,  $R_R$ ,  $R_P$  and  $\bar{\gamma}$  can be expressed in terms of  $V_T$ ,  $T_f$ ,  $h$  and  $R_T$ , the variables of the system are then:  $\bar{\alpha}$ ,  $\psi$ ,  $\theta$ ,  $\phi$ ,  $V_T$ ,  $T_f$ ,  $h$ ,  $R_T$  and  $\bar{\lambda}$ . Note that  $V_T$ ,  $T_f$ ,  $h$ ,  $R_T$  and  $\bar{\lambda}$  are the parameters which have been fixed in order to set the trajectory of the aircraft.

Using the notation in the "Firefly" manual, the fire control bombing equation is written as:

$$P_C = K \left( \frac{C_{P_W} - D_{TN} \omega_w}{R_{D_2}} \right) \quad (3-5)$$

(Ref 2:26)

where  $P_C$  = Roll rate command

$K$  = System gain

The remaining terms may be written in terms of the geometry inputs previously mentioned.  $C_{P_W}$  is defined in reference 2 as:

$$C_{P_W} = S_{V_u} R_{P_V} \quad (3-6)$$

(Ref 2:21)

where

$$S_{V_u} = \cos \alpha \quad (3-7)$$

(Ref 2:20)

$$R_{P_V} = R_{T_V} - G_V \quad (3-8)$$

(Ref 2:14)

Note that  $u$ ,  $v$  and  $w$  correspond to the  $x$ ,  $y$ , and  $z$  body axes of the aircraft. In order to simplify the above expressions, the ejection velocity of the bomb, the target velocity, and the steady wind velocity have all been assumed to be zero. With the aid of the Euler transformation matrix as defined in chapter two,  $R_{T_V}$  and  $G_V$  may be written as:

$$R_{T_V} = R_T \left[ \cos \bar{\gamma} (\cos \psi \sin \theta \sin \phi - \sin \psi \cos \phi) + \sin \bar{\gamma} \cos \theta \sin \phi \right] \quad (3-9)$$

$$G_V = G \cos \theta \sin \phi \quad (3-10)$$

$D_{TN}$  is expressed as:

$$D_{TN} = \frac{R_P^2 - R_R^2}{2V_T} \quad (3-11)$$

(Ref 2:26)

and needs no further defining since it is already in terms of the geometry inputs.

The term  $\Omega_w$  is defined as:

$$\Omega_w = \frac{s_{V_u} A_V}{V_T} \quad (3-12)$$

(Ref 2:22)

where  $A_V$ , the acceleration in the lateral direction may be written as:

$$A_V = \frac{F_{A_V}}{m} + g_{C_V} + \frac{F_{T_V}}{m} \quad (3-13)$$

Since the engines are aligned along the  $x$  axis,

$$A_V = \frac{F_{A_V}}{m} + g_{C_V} \quad (3-14)$$

For the steady state flight condition where the aircraft is assumed to be in coordinated flight with zero sideslip:

$$\begin{aligned} A_{V_0} &= g_{C_V} \\ &= g_c \cos\theta_0 \sin\phi_0 \end{aligned} \quad (3-15)$$

The last undefined term in the roll rate command equation is  $R_{D_2}$  which is expressed as:

$$R_{D_2} = R_p \sin \bar{\lambda} \quad (3-16)$$

(Ref 2:19)

It should be noted that this fire control bombing law contains the error for the nominal conditions. This error may be expressed as:

$$\text{Error} = C_{PW_0} - D_{TN_0} \Omega_{W_0} \quad (3-17)$$

The terms defining the nonlinear fire control equation are summarized in Table II.

#### Linear Fire Control Law

In order to study the effects of the perturbations on the system, the equations can be linearized so that frequency response analysis may be used. To accomplish this, the variables which are responsible for causing a change in the roll rate command must be determined. The perturbations of interest are the ones which change the velocity vector. These are:  $u$ ,  $\beta$ ,  $\alpha$ ,  $p$ ,  $r$ ,  $\psi$ ,  $\theta$ ,  $\phi$ ,  $\delta_{DT}$  and  $\delta_R$ . Also, as these state variables change, they produce a change in the time of fall and the heading angle  $\bar{\lambda}$ . These changes may be denoted as  $t_f$  and  $\lambda$  respectively. Since  $R_T$  is of a large magnitude, even close to the release point, it has been assumed to be a constant. Also, due to the large

values of  $R_T$  and  $h$ ,  $\bar{\gamma}$  has also been assumed to be unaffected by perturbations. Finally, the magnitude of  $R_p$  is independent of the time of fall to a first order of approximation. (Ref 2:17).

As  $T_f$  and  $\bar{\lambda}$  cannot be considered constants, it is necessary to define these parameters since their perturbations will have an effect on the solution. The equation which governs the time of fall of the bomb for a vacuum is:

$$h = \dot{Z} T_f + \frac{1}{2} g_c T_f^2 \quad (3-18)$$

where  $\dot{Z}$  is the initial vertical velocity in the earth fixed coordinate reference frame. Using the Taylor's series expansion and retaining only the linear terms yields:

$$\Delta h = \dot{Z} T_{f_0} + \dot{Z}_0 t_f + g_c T_{f_0} t_f \quad (3-19)$$

Since we assume  $\Delta h$  is equal to zero,  $t_f$  may be written as:

$$t_f = \frac{-\dot{Z} T_{f_0}}{\dot{Z}_0 + g_c T_{f_0}} \quad (3-20)$$

where  $\dot{Z}$  is determined from the following relationship:

$$\begin{bmatrix} \dot{X} \\ \dot{Y} \\ \dot{Z} \end{bmatrix} = [T]^{-1} \begin{bmatrix} U \\ V_{T_0} \sin \bar{\beta} \\ V_{T_0} \sin \bar{\alpha} \end{bmatrix} \quad (3-21)$$

$$\text{or, } \dot{Z}_0 = -U_0 \sin \theta_0 + V_{T_0} \sin \alpha_0 \cos \theta_0 \cos \phi_0 \quad (3-22)$$

Again, using the Taylor's series expansion the linearized equation for  $\dot{Z}$  is:

$$\dot{z} = u (-\sin\theta_0) + \beta(V_{T_0} \cos\theta_0 \sin\phi_0) + \alpha(W_0 \cos\theta_0 \cos\phi_0) - \theta(U_0 \cos\theta_0 + W_0 \sin\theta_0 \cos\phi_0) - \phi(W_0 \cos\theta_0 \sin\phi_0) \quad (3-23)$$

The angle  $\bar{\lambda}$  is defined as the angle between the velocity vector and  $R_p$ , or:

$$\vec{V}_T \cdot \vec{R}_p = V_T R_p \cos \bar{\lambda} \quad (3-24)$$

The roll rate command equation may now be linearized by taking the Taylor's series expansion of the equations for:  $T_f$ ,  $\bar{\lambda}$ ,  $C_{p_w}$ ,  $D_{TN}$ ,  $\Omega_w$ ,  $R_{D_2}$ , and  $P_c$ . Their respective values for each of the perturbed variables are defined in Fig. 21. (Elements (14,1) through (20,5)).

The roll rate command is then passed through an integrator to obtain a bank angle steering bar. This step is accomplished since the literature refers to roll task models where the bank angle is being controlled and not the roll rate.

Table II

Summary of Nonlinear Fire Control Law

Fixed Parameters

$g_c$   $K_D$   $V_{T_0}$   $\rho/\rho_0$   $T_{f_0}$   $R_{T_0}$   $h$   $\bar{\lambda}_0$

Input State Variables

$\bar{\alpha}$

$\psi$

$\theta$

$\phi$

$$D_p = 1 - K_D \rho / \rho_0 V_T T_f$$

$$G = .5 D_p g_c T_f^2$$

$$R_R = D_p g_c T_f^2$$

$$\bar{\gamma} = \sin^{-1} \left( \frac{h}{R_T} \right)$$

$$R_P = R_T \cos \left[ \tan^{-1} \left( \frac{G \cos \gamma}{R_T - G \sin \gamma} \right) \right] - \left\{ G^2 - \right.$$

$$\left. R_T^2 \sin^2 \left[ \tan^{-1} \left( \frac{G \cos \gamma}{R_T - G \sin \gamma} \right) \right] \right\}^{1/2}$$

$$R_{T_V} = R_T \cos \bar{\gamma} (\cos \psi \sin \theta \sin \phi - \sin \psi \cos \phi) +$$

$$R_T \sin \bar{\gamma} \cos \theta \sin \phi$$

$$G_V = G \cos \theta \sin \phi$$

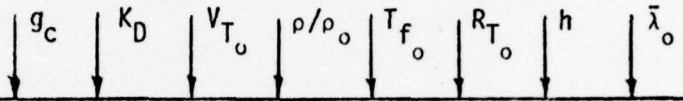
$$D_{TN} = \frac{R_P^2 - R_R^2}{2V_T}$$

$$C_{P_w} = \cos \bar{\alpha} (R_{T_V} - G_V)$$

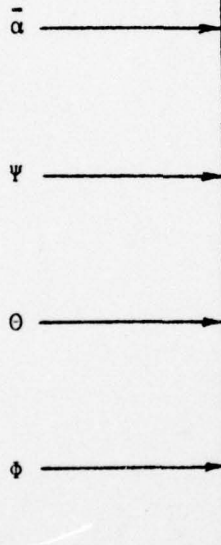
Table II (Continued)

Summary of Nonlinear Fire Control Law

Fixed  
Parameters



Input  
State  
Variables



$$\Omega_w = \frac{g_c \cos \theta \sin \phi \cos \bar{\alpha}}{V_T}$$

$$R_{D2} = R_p \sin \bar{\lambda} - \dot{z} + (\dot{z}^2 + 2g_c h)^{\frac{1}{2}}$$

$$T_f = \frac{-g_c}{-g_c}$$

$$\bar{\lambda} = \cos^{-1} \left( \frac{\vec{V}_T \cdot \vec{R}_p}{V_T R_p} \right)$$

$$P_c = K \left( \frac{C_{Pw} - D_{TN} \Omega_w}{R_{D2}} \right)$$

#### IV. Turbulence Response Model

To determine the aircraft response to wind gusts, it is necessary to represent the atmospheric turbulence by mathematical models. This can be done by representing the wind gusts as input power spectral densities (PSD). It is assumed here that the turbulence is isotropic, homogeneous and of a stationary nature for altitudes above 1750 feet AGL. (Ref 3:419-421). The input PSD can then be represented as:

$$\text{PSD}_{IN} = \phi_{i_g} = |T_{i_g}(\omega)|^2 D \quad (4-1)$$

where  $T_{i_g}(\omega)$  is the transfer function describing the shaping filter which transforms white noise of intensity  $D$  into colored noise representing the wind gusts for that particular direction. The PSDs for the wind gusts along the lateral and vertical axes are represented by  $\phi_{v_g}$  and  $\phi_{w_g}$  while the PSDs for the wind gusts angular velocities about the roll, pitch, and yaw axes are represented by  $\phi_{p_g}$ ,  $\phi_{q_g}$ , and  $\phi_{r_g}$ . For the purpose of this analysis, the intensity or rms value of the white noise ( $D$ ) may be assumed to be unity.

The Dryden spectral form of the turbulence will be used in this analysis since it is a simpler model. For flying qualities analysis, the Dryden model yields essentially the same results as the more complicated VonKarman model (Ref 3:422). The Dryden form for the continuous random models are:

$$\phi_{v_g}(\omega) = \frac{\sigma_v^2 L_v \left[ 1 + 3 \left( \frac{L_v \omega}{V_{T_0}} \right)^2 \right]}{V_{T_0} \pi \left[ 1 + \left( \frac{L_v \omega}{V_{T_0}} \right)^2 \right]^2} \quad (4-2)$$

$$\phi_{Wg}(\omega) = \frac{\sigma_w^2 L_w \left[ 1 + 3 \left( \frac{L_w \omega}{V_{T_o}} \right)^2 \right]}{V_{T_o} \pi \left[ 1 + \left( \frac{L_w \omega}{V_{T_o}} \right)^2 \right]^2} \quad (4-3)$$

$$\phi_{Pg}(\omega) = \frac{\sigma_w^2 (0.8) \left( \frac{\pi L_w}{4b} \right)^{1/3}}{V_{T_o} L_w \left[ 1 + \left( \frac{4b \omega}{\pi V_{T_o}} \right)^2 \right]} \quad (4-4)$$

$$\phi_{Qg}(\omega) = \frac{\omega^2 \phi_{Wg}(\omega)}{V_{T_o}^2 \left[ 1 + \left( \frac{4b \omega}{\pi V_{T_o}} \right)^2 \right]} \quad (4-5)$$

$$\phi_{Rg}(\omega) = \frac{\omega^2 \phi_{Vg}(\omega)}{V_{T_o}^2 \left[ 1 + \left( \frac{3b \omega}{\pi V_{T_o}} \right)^2 \right]} \quad (4-6)$$

(Ref 3:459,460)

where  $\sigma_i$  = The root-mean square intensity of the wind gusts.

$L_i$  = Scaling factor for the wind gust.

$\omega$  = Frequency in radians/second.

$b$  = Wing span of the aircraft.

Since the  $u_g$  has little effect on high speed aircraft due to their high momentum,  $\phi_{u_g}$  is not considered in this analysis.

For the clear air turbulence model, the scales for the Dryden form are:

$$L_u = L_v = L_w = 1750 \text{ feet} \quad (4-7)$$

(Ref 3:444)

for altitudes above 1750 feet above the terrain. The root-mean-square

intensity  $\sigma_w$  is defined as approximately six feet per second for altitudes around 2500 feet above the terrain. The intensities  $\sigma_u$  and  $\sigma_v$  may then be obtained from the following relationship:

$$\frac{\sigma_u^2}{L_u} = \frac{\sigma_v^2}{L_v} = \frac{\sigma_w^2}{L_w} \quad (4-8)$$

(Ref 3:435)

This results in the three intensities being equal or  $\approx 6$  feet/second. Noting that  $q_g$  and  $w_g$  are correlated, it is possible to represent

$\phi_{q_g}$  as:

$$\phi_{q_g}(\omega) = |T_{q_g}(j\omega)|^2 \cdot \phi_{w_g}(\omega) \quad (4-9)$$

where

$$T_{q_g}(s) = \frac{\frac{s}{V_{T_o}}}{1 + \frac{4bs}{\pi V_{T_o}}} \quad (4-10)$$

Likewise,  $\phi_{r_g}$  and  $\phi_{v_g}$  are correlated, where  $\phi_{r_g}$  may be represented as:

$$\phi_{r_g}(\omega) = |T_{r_g}(j\omega)|^2 \cdot \phi_{v_g}(\omega) \quad (4-11)$$

where

$$T_{r_g}(s) = \frac{-\frac{s}{V_{T_o}}}{1 + \frac{3bs}{\pi V_{T_o}}} \quad (4-12)$$

(Ref 3:459-460)

Since the equations describing the basic aircraft are in terms of  $\alpha$  and  $\beta$ , it should be noted that:

$$\phi_{\alpha_g}(\omega) = |T_{\alpha_g}|^2 \cdot \phi_{w_g} \quad (4-13)$$

$$\phi_{\beta g}(\omega) = |T_{\beta g}|^2 \cdot \phi_{v_g} \quad (4-14)$$

where

$$T_{\alpha g} = T_{\beta g} = \frac{1}{V_{T_o}} \quad (4-15)$$

(Ref 3:421)

The three power spectral densities,  $\phi_{v_g}$ ,  $\phi_{w_g}$ , and  $\phi_{p_g}$ , which are the uncorrelated inputs to the system are plotted in figures 7 and 8.

Since  $\sigma_v$  is equal to  $\sigma_w$  and  $L_v$  is equal to  $L_w$ ,  $\phi_{v_g}$  is equal to  $\phi_{w_g}$ .

To analyze the response of a system to an input PSD, it is necessary to obtain the output PSD which is:

$$\text{PSD}_{\text{OUT}} = |G(j\omega)|^2 \cdot \text{PSD}_{\text{in}} \quad (4-16)$$

where  $G(j\omega)$  is the open loop transfer function of the system being analyzed.  $G(j\omega)$  is determined by replacing all the linear and angular velocities in the aerodynamic terms of the aircraft equations with the following:

$$U_A = U + U_g \qquad p_A = p + p_g$$

$$\beta_A = \beta + \beta_g \qquad q_A = q + q_g$$

$$\alpha_A = \alpha + \alpha_g \qquad r_A = r + r_g$$

These wind gust components are then treated as inputs to the system.

In matrix form, the system equations may be written as:

$$\begin{aligned} [A] [R] = [B_o] F_{AS} + [B_1] \beta_g + [B_2] \alpha_g + [B_3] p_g + \\ [B_4] q_g + [B_5] r_g \end{aligned} \quad (4-17)$$

where  $[A]$  - Matrix which defines the system components.

- $[R]$  - The vector representing perturbation variables.  
 $[B_i]$  - The vector which represents the inputs to the system.

(See Appendix D for a more complete explanation).

For a wind gust  $[B_0]$  is zero. Also, since  $\beta_g$  and  $r_g$ , and  $\alpha_g$  and  $q_g$  are correlated, they may be combined as:

$$[B] = [B_1 \cdot T_{\beta_g} + B_5 \cdot T_{r_g}] + [B_2 \cdot T_{\alpha_g} + B_4 \cdot T_{q_g}] + [B_3] \quad (4-18)$$

for the power spectral density inputs  $\phi_{v_g}$ ,  $\phi_{w_g}$ , and  $\phi_{p_g}$  respectively. To simplify the description for these combined inputs, the wind gusts which are related to the  $\phi_{v_g}$  inputs will be called lateral gusts, while the  $\phi_{w_g}$  inputs will be referred to as longitudinal gusts and the  $\phi_{p_g}$  inputs will be annotated as P gusts or roll gusts. The combined effect of these three gusts will be referred to as a composite gust. The value of the composite gust may be calculated by summing the squared values for each of the three individual gusts and then taking the square root of the sum. Figure 23 in Appendix D presents the B matrix as defined in the computer program used for this study. These wind gust inputs originate in the force and moment equations of the aircraft and the flight control equations where  $f_{A_y}$  and  $f_{A_z}$  are fed back into the pitch and yaw axis equations. Figure 24 in Appendix D represents the B matrix where the flight controls have been modified for the automatic fire control system. The P parameter which controls the sequence of the inputs is also defined in Appendix D.

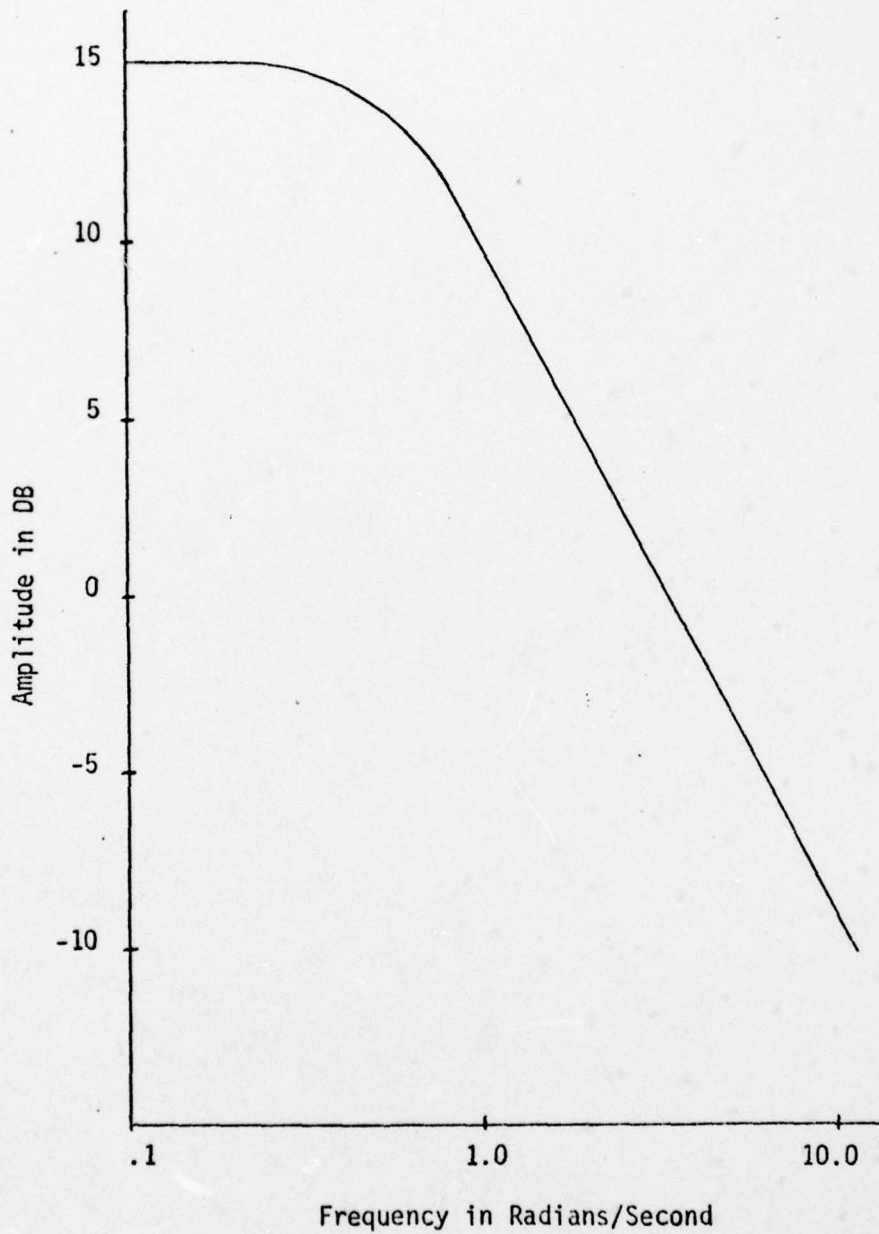


Fig. 7. Input PSD for Lateral and Vertical Gusts

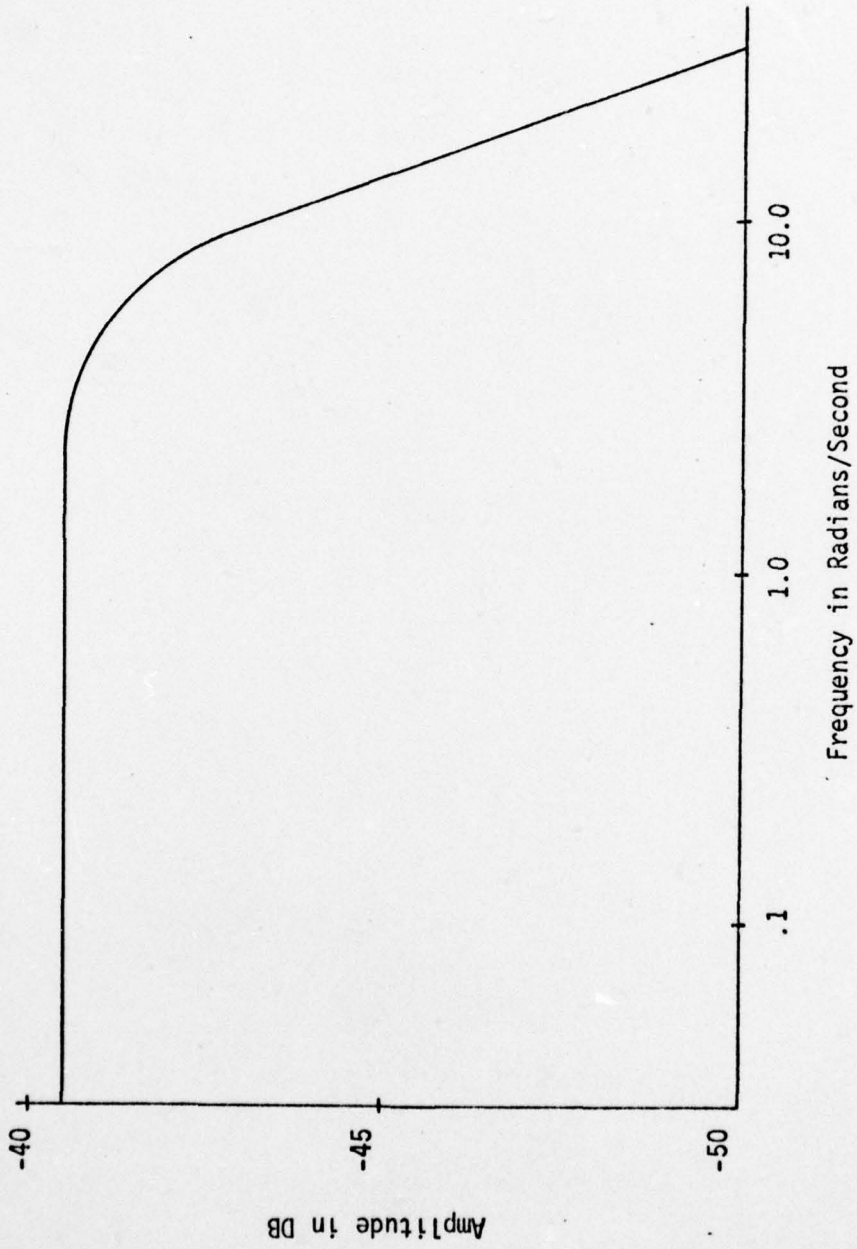


Fig. 8. Input PSD for P Gusts

## V. Pilot Model

### Background

In recent years a great deal of work has been done in an attempt to represent the human pilot by an analytical model. These pilot models are used in conjunction with system models to form predictions or explain the behavior of the closed loop system where the pilot closes the loop. Systems Technology, Inc. has been prominent in developing different pilot models and the reader is referred to reference 4 for a thorough discussion of the topic. The general model developed in reference 4 is given in its simplified form as:

$$Y_p = K_p e^{-j\omega\tau} \left( \frac{T_L j\omega + 1}{T_I j\omega + 1} \right) \left( \frac{1}{T_N j\omega + 1} \right) \quad (5-1)$$

(Ref 4:17)

where  $K_p$  = Pilot gain

$e^{-j\omega\tau}$  = Transport delay due to basic latencies such as nerve condition, data processing, etc.

$\left( \frac{T_L j\omega + 1}{T_I j\omega + 1} \right)$  = Pilot adjustment parameters and equalization characteristics the pilot will adopt to suit the task.

$\left( \frac{1}{T_N j\omega + 1} \right)$  = First order neuromuscular lag terms.

This model can be simplified still further by combining the transport delay due to basic latencies with the neuromuscular system lag term. This combination is often referred to as the effective time delay,  $\tau_e$ .

These simplifications lead to the more commonly used model:

$$Y_p = K_p \left( \frac{T_L s + 1}{T_I s + 1} \right) e^{-\tau_e s} \quad (5-2)$$

(Ref 5:234)

where  $j\omega = s$  for continuous random like inputs.

#### Crossover Model

The pilot-vehicle models are most useful for compensatory tracking tasks where the pilot acts upon a displayed error due to some random input. The transfer function describing the controlled element is  $Y_c(s)$  while the pilot's control action which is linearly correlated with the input is described by  $Y_p(s)$ . In order to minimize the error, the amplitude ratio of the open loop frequency response,  $|Y_{OL}| = Y_p Y_c$ , should be very large over the frequency of the input band width and very small outside this range. (Ref 5:233).

The pilot attempts to achieve this condition by adopting sufficient lead or lag equalization so that the slope of  $|Y_{OL}|$  lies very close to -20 dB/decade in the region of crossover frequency,  $\omega_c$ . This crossover frequency occurs where  $|Y_{OL}| = 1.0$  or 0 dB. For small tracking errors,  $\omega_c$  should be greater than the input frequency,  $\omega_i$ . The pilot can adjust this crossover frequency by adjusting his gain,  $K_p$ . This leads to the "two parameter crossover model which can account for most of the significant open loop data trends in the important crossover frequency region. The crossover model is:

$$Y_{OL}(s) = Y_p Y_c = \frac{\omega_c e^{-\tau_e s}}{s} \quad (5-3)$$

near  $\omega_c$ ." (Ref 5:234). Here,  $\omega_c$  is equivalent to the pilot or loop gain while  $\tau_e$  represents the lead or lag induced by the pilot. If the form of  $Y_c$  is known,  $Y_p$  can be determined from:

$$Y_p = \frac{\omega_c e^{-\tau} e^s}{s Y_c} \quad (5-4)$$

In reference 5, typical aircraft control tasks have been determined where:

$$Y_c \approx \frac{K_c}{s(Ts + 1)} \quad (5-5)$$

represents the roll angle being controlled by lateral stick inputs (Ref 5:236).  $Y_p$  can then be written as:

$$Y_p = K_p (T_L s + 1) e^{-\tau} e^s \quad (5-6)$$

This indicates that a typical system would show a - 40 dB/decade slope in the region prior to the crossover frequency. The pilot then adds enough lead to make the slope in this region - 20 dB/decade.

In reference 6, an analysis was conducted where the roll task was studied with regards to pilot models. In this same report, it was determined that the pilot model could be represented as:

$$Y_p = K_p (.5 s + 1) e^{-.3s} \quad (5-7)$$

for the roll task which consisted of attempting to maintain a fixed bank angle in a turbulent field (Ref 6.12).

The pilot model represented in equation (5-7) is the model used in this thesis. The reasons for this choice are:

1. The same task is being accomplished.
2. The inputs to the system are modeled as turbulence.

The pilot gain is determined by placing the crossover frequency at approximately four radians per second for an open loop controlled system with a - 40 dB slope prior to the crossover point (Ref 5:237).

System Application

The pilot model can be added to the system as shown in figure 9.

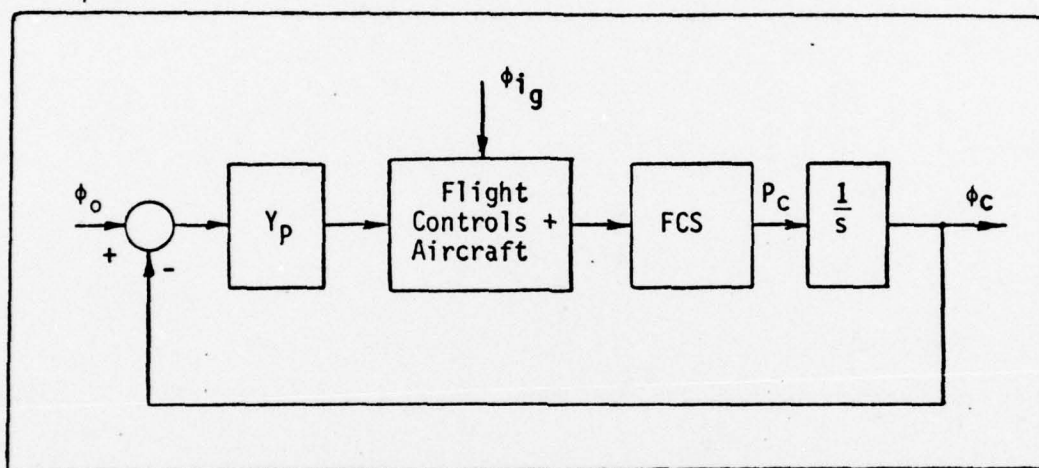


Fig. 9. Closed Loop System with Pilot Model

The reference angle  $\phi_o$  may be set equal to zero since  $\phi_c$  represents the perturbations about this reference bank angle. With this simplification the pilot's horizontal stick inputs can be written as:

$$F_{AS} = Y_p (\phi_o - \phi_c)$$

$$= - \left[ K_p (.5s + 1)e^{-.3} \right] \frac{p_c}{s} \tag{5-8}$$

where  $\phi_c$  is equal to  $p_c/s$ .

With these inputs, the primary roll axis equations in Appendix C can now be written as:

$$\delta_A (23.87) + \frac{P_C}{s} \left[ K_p (.5s + 1)e^{-.3s} \right] = 0 \quad (5-9)$$

$$p(.0625) + \delta_{DT}(2) + \frac{P_C}{s} \left[ K_p (.5s + 1)e^{-.3s} \right] \left( \frac{.0019s + .0074}{.3s + 1} \right) = 0 \quad (5-10)$$

For the basic aircraft, the pilot model will be attempting to null the perturbation roll angle  $\phi$ . The primary roll axis equations will be the same as the above except that  $\frac{P_C}{s}$  is replaced by  $\phi$ .

## VI. System Evaluation and Results

The preceding chapters along with the appendices develop the equations which define the system and describe the computer program to solve for the frequency response. The purpose of this chapter is to evaluate those areas which will indicate how the system responds to random inputs and to compare these responses for different configurations of the system.

### Form of $Y_C$

The first item to be considered is the form of the transfer function  $Y_C$  for the complete system including the fire control system. Figure 10 shows the Bode plot asymptotes for the basic aircraft and the complete system where the input is an aileron deflection of unit magnitude. The output is  $\phi_C$  for the complete system and  $\phi$  for the basic aircraft. Recalling from chapter 5, the pilot must adjust his lead or lag to achieve a -20 dB/decade slope for the combined  $Y_P Y_C$  response for a good portion of the region prior to the crossover frequency. He then adjusts his gain to place the crossover frequency somewhere around 4 radians/second. For the basic aircraft, all the pilot needs to do is adjust his gain since this system, which already demonstrates a -20 dB slope, needs no further equalization. For the complete system the pilot must not only adjust his gain but he must also add some lead to reduce the -40 dB/decade slope to approximately -20 dB/decade. The pilot model which was chosen in chapter 5 is capable of producing the desired slope of -20 dB/decade by adding the .5 seconds of lead time. This only

leaves the pilot gain to be adjusted so as to achieve the desired cross-over frequency.

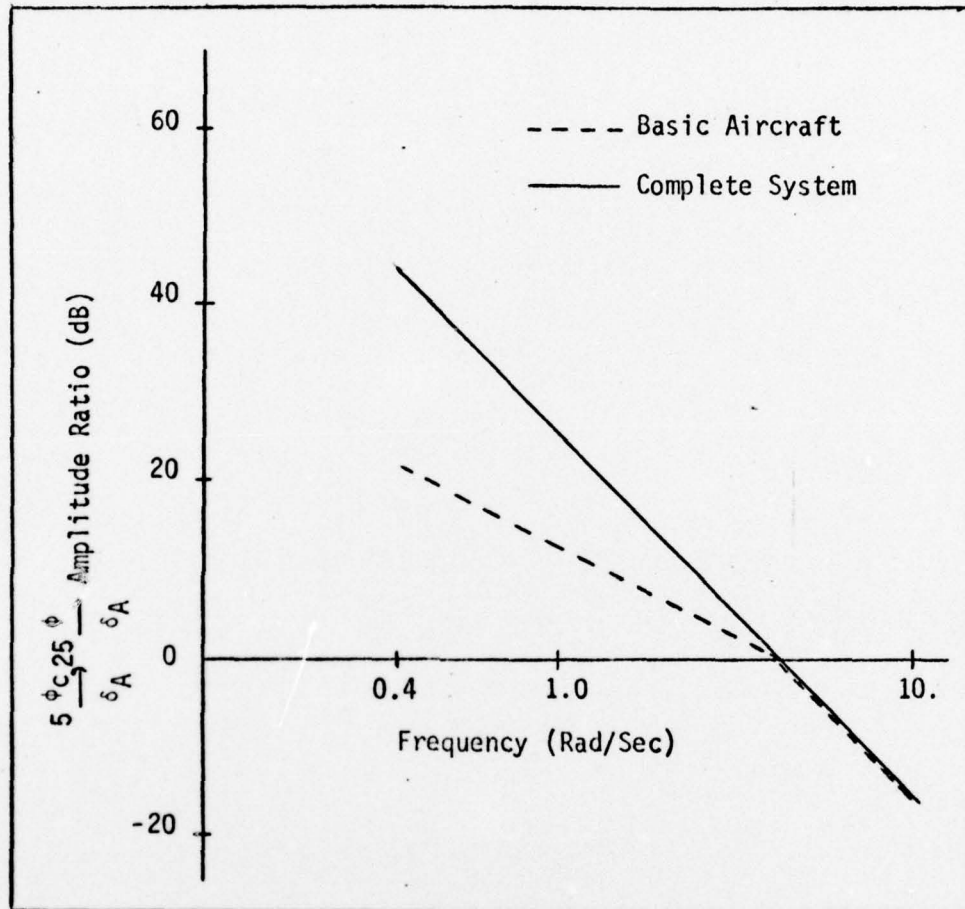


Fig. 10. System Response to a Unit Lateral Input

#### Pilot Gain

The pilot gain for this system is measured as pounds/radian. As the pilot gain is increased, the crossover frequency increases resulting in a larger bandwidth. The pilot gain for the different configurations and different trajectories is determined by increasing

the open loop system gain to achieve a crossover frequency of approximately 4 radians/second. The pilot then adopts this gain so as to maintain the same crossover frequency for the closed loop system. Table III shows the required pilot gains to achieve a crossover frequency of approximately 4 radians/second. It should be noted that for the basic aircraft, the pilot gain is independent of bank angle. However, for the case where the pilot is following the command bank angles as displayed on the HUD, the pilot gain increases as the bank angle increases. This characteristic does not have any significant influence on the pilot rating, since it is easily compensated for by the pilot.

Table III  
Pilot Gain

<u>Flight Condition</u>	$K_p^*$ for $\phi$	$K_p^*$ for $\phi_c$
Straight and level	25	5
Level turn	25	80
Descending turn	25	80

\*  $\omega_c \approx 4$  rad/sec

RMS Values for  $\phi_c$  and  $\phi$

In order to analyze the bank angle system response, three types of trajectories were considered:

1. Straight and level flight (the aircraft heading remains aligned with the target while maintaining a constant altitude of 2500 feet above the target).

2. Level turn (the initial aircraft heading is  $30^\circ$  off the target at a slant range of 12,000 feet while maintaining a constant altitude of 2500 feet above the target).
3. Descending turn (the initial aircraft heading is again  $30^\circ$  off the target at a slant range of 12,000 feet and in a shallow descent of approximately  $10^\circ$ ).

With random wind gusts as inputs, each of these trajectories are evaluated to determine the rms values for  $\phi_C$  and  $\phi$ . This is done for the following configurations:

1. Basic aircraft (no pilot and no fire control system), see Table IVa.
2. Basic aircraft with pilot closing the loop by trying to null the  $\phi$  perturbations, see Table IVb.
3. Aircraft plus fire control system (no pilot), see Table Va.
4. Aircraft plus fire control system with pilot closing the loop by trying to null the  $\phi_C$  perturbations, see Table Vb and Vc.
5. Fire control system output signal fed directly to the F-15 flight controls, see Table VIa and VIb.

Tables IV, V and VI summarize the rms values for  $\phi$  and  $\phi_C$  which are in degrees. Comparing Table IVa and Table Vc, it is interesting to note that in two of the three cases, the perturbed bank angle rms values for the closed loop system actually increased over the open loop system even though the pilot was able to essentially null the perturbed error signal. Table IV indicates that the pilot is much more successful at reducing the rms perturbed bank angle values by trying to null  $\phi$  instead of  $\phi_C$ . When  $\sigma_{\phi_C}$  for the automatic system is compared to  $\sigma_{\phi_C}$  for the manual system, it is obvious that the pilot is better able to null the

error signal than the flight controls. However, the perturbed bank angle is generally greater for the pilot than the autopilot. As a final observation, it can be noted that the open loop  $\sigma_{\phi_C}$  is extremely large inferring the system will direct large bank angle commands if the perturbations are allowed to go unattended. The probable cause for the high degree of sensitivity for the straight and level case is the denominator of the bombing equation (Eq. 3-5) becomes very small as  $\lambda$  goes to zero.

Table IV

Bank Angle Response for Aircraft without Fire Control System

a.  $\sigma_{\phi_{OL}}$  - RMS Value for Open Loop Perturbed Bank Angle

Type Gust	<u>Straight &amp; Level</u>	<u>Level Turn</u>	<u>Descending Turn</u>
Lateral	1.33	1.70	1.47
Vertical	.01	.21	.13
P	1.33	1.67	1.63
Composite	1.93	2.41	2.27

b.  $\sigma_{\phi_{CL}}$  - RMS Value for Closed Loop Perturbed Bank Angle

Type Gust	<u>Straight &amp; Level</u>	<u>Level Turn</u>	<u>Descending Turn</u>
Lateral	.43	.57	.49
Vertical	.0	.01	.01
P	.18	.19	.19
Composite	.47	.61	.53

RMS Values are in Degrees.

Table V

Bank Angle Response for Aircraft with Fire Control System and Pilot

a.  $\sigma_{\phi_{COL}}$  - RMS Value for Open Loop Perturbed Command Bank Angle

<u>Type Gust</u>	<u>Straight &amp; Level</u>	<u>Level Turn</u>	<u>Descending Turn</u>
Lateral	Limit	7.96	14.16
Vertical	3.44	3.84	3.33
P	Limit	34.44	30.25
Composite	Limit	39.03	38.86

b.  $\sigma_{\phi_{CCL}}$  - RMS Value for Closed Loop Perturbed Command Bank Angle

<u>Type Gust</u>	<u>Straight &amp; Level</u>	<u>Level Turn</u>	<u>Descending Turn</u>
Lateral	5.12	.03	.11
Vertical	.01	.01	.01
P	.64	.04	.04
Composite	5.15	.05	.11

c.  $\sigma_{\phi_{CL}}$  - RMS Value for Closed Loop Perturbed Bank Angle

<u>Type Gust</u>	<u>Straight &amp; Level</u>	<u>Level Turn</u>	<u>Descending Turn</u>
Lateral	5.83	2.19	3.16
Vertical	.01	.15	.11
P	.08	.09	.09
Composite	5.84	2.19	3.16

RMS Values are in Degrees.

Table VI

Bank Angle Response where Fire Control System  
is Connected to the Flight Controls

a.  $\sigma_{\phi_c}$  - RMS Value for Perturbed Command Bank Angle

<u>Type Gust</u>	<u>Straight &amp; Level</u>	<u>Level Turn</u>	<u>Descending Turn</u>
Lateral	6.02	2.89	3.28
Vertical	.01	.19	.19
P	.3	.25	.24
Composite	6.05	2.95	3.36

b.  $\sigma_{\phi}$  - RMS Value for Perturbed Bank Angle

<u>Type Gust</u>	<u>Straight &amp; Level</u>	<u>Level Turn</u>	<u>Descending Turn</u>
Lateral	4.81	2.17	2.76
Vertical	.01	.17	.13
P	.10	.26	.25
Composite	4.83	2.19	2.78

### Error Analysis

The distance the bomb misses the target is an excellent measure for determining if a bombing system is of any use. Since the solution for this fire control system is being continually updated, only the perturbations injected into the system at the time of release will result in an error. This error or miss distance is related to the difference between the magnitude and orientation of the perturbed velocity vector and the nominal velocity vector. Since the miss distance is measured in the earth fixed coordinate system, it is

advantageous to use the Euler transformation matrix as follows:

$$\begin{bmatrix} \dot{X} \\ \dot{Y} \\ \dot{Z} \end{bmatrix} = [T]^{-1} \begin{bmatrix} U \\ V_{T_0} \sin \bar{\beta} \\ V_{T_0} \sin \bar{\alpha} \end{bmatrix}$$

where  $\dot{X}$ ,  $\dot{Y}$  and  $\dot{Z}$  are total velocities in the earth fixed reference frame. The  $\dot{X}$ ,  $\dot{Y}$  and  $\dot{Z}$  equations may be written as:

$$\begin{aligned} \dot{X} = U (\cos \psi \cos \theta) + V_{T_0} \sin \bar{\beta} (\cos \psi \sin \theta \sin \phi - \sin \psi \cos \phi) + \\ V_{T_0} \sin \bar{\alpha} (\cos \psi \sin \theta \cos \phi + \sin \psi \sin \phi) \end{aligned} \quad (6-1)$$

$$\begin{aligned} \dot{Y} = U (\sin \psi \cos \theta) + V_{T_0} \sin \bar{\beta} (\sin \psi \sin \theta \sin \phi + \cos \psi \cos \phi) + \\ V_{T_0} \sin \bar{\alpha} (\sin \psi \sin \theta \cos \phi - \cos \psi \sin \phi) \end{aligned} \quad (6-2)$$

$$\dot{Z} = U (-\sin \theta) + V_{T_0} \sin \bar{\beta} (\cos \theta \sin \phi) + V_{T_0} \sin \bar{\alpha} (\cos \theta \cos \phi) \quad (6-3)$$

where the above variables include the steady state and perturbed quantities. By using the Taylor's series expansion and retaining only the linear terms, the expressions defining the perturbation values of  $\dot{x}$ ,  $\dot{y}$  and  $\dot{z}$  may be determined.

The lateral error may then be written as

$$e_y = \dot{y} (t_{f_0} + t_f) \quad (6-4)$$

and the longitudinal error may be written as

$$e_x = \dot{x} (t_{f_0} + t_f) + U_0 t_f \quad (6-5)$$

Neglecting the products of the perturbations, the lateral and longitudinal errors may be written as:

$$e_y = \dot{y} t_{f_0} \quad (6-7)$$

$$e_x = \dot{x} t_{f_0} + U_0 t_f \quad (6-8)$$

The total error may be written as:

$$e_r = (e_y^2 + e_x^2)^{\frac{1}{2}} \quad (6-9)$$

Again using the random wind gusts as inputs, power spectral density analysis can be performed to calculate a rms miss distance based upon the preceding equations. Tables VII, VIII and IX show the average miss distances for the different trajectories and different configurations defined in the last section. From these tables, it can be seen that:

1. The P wind gust component does not produce significant miss distances.
2. The lateral wind gusts are mainly responsible for the lateral errors for straight and level flight.
3. The vertical wind gusts are mainly responsible for the longitudinal errors for straight and level flight.
4. The lateral wind gusts have a large effect on the longitudinal error for turning flight since a lateral perturbation causes the velocity vector to be perturbed in the vertical plane as well as the horizontal plane.
5. The vertical wind gusts have a significant effect on the lateral error for turning flight since a pitching perturbation causes the velocity vector to be perturbed in the horizontal plane as well as the vertical plane.
6. The miss distances are significantly reduced when the aircraft is flying in a descending turn because of the reduced time of fall of the bomb.

Table VII  
 Error Analysis for Aircraft without Fire Control System  
 (Pilot Nulls  $\phi$ )

a.  $\sigma_{e_x}$  - RMS Value for Longitudinal Error

<u>Type Gust</u>	<u>Straight &amp; Level</u>	<u>Level Turn</u>	<u>Descending Turn</u>
Lateral	.3	18.	7.
Vertical	101.	54.	41.
P	.2	7.	2.
Composite	101.0	59.	42.

b.  $\sigma_{e_y}$  - RMS Value for Lateral Error

<u>Type Gust</u>	<u>Straight &amp; Level</u>	<u>Level Turn</u>	<u>Descending Turn</u>
Lateral	8.	6.	3.
Vertical	1.	51.	15.
P	2.	5.	1.
Composite	9.	56.	16.

c.  $\sigma_{e_T}$  - RMS Value for Total Error

<u>Type Gust</u>	<u>Straight &amp; Level</u>	<u>Level Turn</u>	<u>Descending Turn</u>
Lateral	8.	19.	8.
Vertical	101.	64.	41.
P	2.	9.	2.
Composite	102.	71.	42.

RMS Values are in Feet.

Table VIII

Error Analysis where Pilot Nulls  $\phi_c$

a.  $\sigma_{e_x}$  - RMS Value for Longitudinal Error

Type Gust	<u>Straight &amp; Level</u>	<u>Level Turn</u>	<u>Descending Turn</u>
Lateral	7.	101.	40.
Vertical	101.	45.	39.
P	.1	1.	.3
Composite	101.	111.	56.

b.  $\sigma_{e_y}$  - RMS Value for Lateral Error

Type Gust	<u>Straight &amp; Level</u>	<u>Level Turn</u>	<u>Descending Turn</u>
Lateral	91.	57.	34.
Vertical	2.	39.	14.
P	.3	.3	.2
Composite	91.	69.	37.

c.  $\sigma_{e_T}$  - RMS Value for Total Error

Type Gust	<u>Straight &amp; Level</u>	<u>Level Turn</u>	<u>Descending Turn</u>
Lateral	91.	114.	50.
Vertical	101.	53.	39.
P	.4	1.	.3
Composite	137.	128.	64.

RMS Values are in Feet.

Table IX  
 Error Analysis where Fire Control System  
 is Connected to the Autopilot

a.  $\sigma_{e_x}$  - RMS Value for Longitudinal Error

<u>Type Gust</u>	<u>Straight &amp; Level</u>	<u>Level Turn</u>	<u>Descending Turn</u>
Lateral	13.	127.	73.
Vertical	104.	45.	39.
P	0.	4.	1.
Composite	105.	135.	83.

b.  $\sigma_{e_y}$  - RMS Value for Lateral Error

<u>Type Gust</u>	<u>Straight &amp; Level</u>	<u>Level Turn</u>	<u>Descending Turn</u>
Lateral	75.	56.	35.
Vertical	1.	28.	8.
P	0.1	2.	1.
Composite	75.	63.	36.

c.  $\sigma_{e_T}$  - RMS Value for Total Error

<u>Type Gust</u>	<u>Straight &amp; Level</u>	<u>Level Turn</u>	<u>Descending Turn</u>
Lateral	73.	137.	76.
Vertical	104.	47.	39.
P	0.3	4.	1.
Composite	128.	147.	87.

RMS Values are in Feet.

Since it is difficult to tell exactly which perturbations are responsible for the miss distances, a computer run was made for the level turn case to determine the significant perturbations. Table X is a listing of the rms values for each perturbed quantity which enters into the error equation. For the lateral error,  $\beta$  and  $\psi$  are the two main contributors to the miss distance while  $t_f$  is the major contributor to longitudinal error with  $u$  contributing about 20%.

Table X  
RMS Values for Error Parameters (Level Turn)

<u>Variable</u>	<u>Lateral Gust</u>	<u>Vertical Gust</u>	<u>P Gust</u>
$\sigma_u$ (ft)	1.67	2.29	.01
$\sigma_\beta$ (deg)	.48	.0	.0
$\sigma_\alpha$ (deg)	.04	.34	.0
$\sigma_\psi$ (deg)	.27	.33	.0
$\sigma_\theta$ (deg)	.39	.14	.01
$\sigma_\phi$ (deg)	2.00	.14	.08
$\sigma_{t_f}$ (sec)	.15	.05	.0

#### Pilot Workload

The last area to be considered to determine if the pilot is capable of manually accomplishing the bomb run is to determine the Cooper-Harper rating for the task. The Cooper-Harper rating is a function of performance, pilot lead and aircraft response. Reference 7 derives an equation which assigns a number to this pilot rating for the roll task being considered in this study.

$$PR = R_1 (\text{Perf}) + R_2 (T_L) + R_3 \left( \frac{\omega_\phi}{\omega_d} \right) + 1 \quad (6-10)$$

(Ref 7:16)

where PR = Pilot Rating

$R_1 (\text{Perf})$  = Performance Contribution

$$= 1.31 \sigma_{\phi_C} + \sigma_{\beta_g} - 1$$

$R_2 (T_L)$  = Pilot work load due to lead time.

$$= 3.25 (1 - e^{-.769 T_L})$$

$R_3 \left( \frac{\omega_\phi}{\omega_d} \right)$  = Ratio of undamped natural frequency of numerator quadratic of  $\phi/\delta_A$  and undamped natural frequency of the dutch roll oscillation.

$$= 6.66 \left( 1 - \frac{\omega_\phi}{\omega_d} \right)$$

For the F-15 aircraft,  $\omega_\phi/\omega_d$  is equal to 1.04 for the flight conditions used in this report. For the pilot model described in chapter 5, the pilot must generate a lead time of 0.5 seconds. The lateral wind gust defined in chapter 4 sets  $\sigma_{\beta_g}$  equal to .52 degrees. The last parameter required to solve for the pilot rating is  $\sigma_{\phi_C}$ . These rms values are tabulated in Table V where the pilot attempts to null the command bank angle  $\phi_C$ . For the descending turn case,  $\sigma_{\phi_C}$  is equal to .0115 degrees. The pilot rating for this run is determined to be 2 where system characteristics are defined to be good and pilot compensation is not a factor to achieve the desired performance. For the straight and level trajectory where  $\sigma_{\phi_C}$  is equal to 5.15°, the pilot rating is determined to be 8.5. This rating indicates there are major deficiencies in the system and that considerable pilot compensation is required for aircraft

control. (Ref 3.19).

## VII. Conclusions

If a pilot is to be considered capable of releasing a weapon in a turn, he must be able to act upon the controlled element in such a way so as to substantially reduce the error signal without causing an undue work load upon himself. The transfer function  $Y_C$  indicates, that with sufficient gain, the simple, single axis pilot model which was chosen in chapter 5 is able to accomplish this roll task. The pilot gains encountered in this study are not excessive and should not be a factor in determining the pilots workload. The .5 seconds lead time and the .3 seconds pure time delay are well within the normal response times for a pilot.

The pilot model is very effective at nulling the errors in  $\phi_C$  due to wind gust inputs. In fact, the pilot model does a better job of nulling the error signal than the automated fire control system which ties in directly to the flight controls. While reducing the error signal  $\phi_C$ , the pilot tends to generate a larger perturbed bank angle than the automated system. This indicates that the pilot inputs are not as smooth or efficient as those through the automated system. However, it should be noted that the miss distances, as a result of the larger perturbations in  $\phi$ , are small when compared to the miss distances caused by  $\psi$ ,  $\beta$ , and  $t_f$ .

The miss distances for the fully automated system and the manual system are comparable. However, it should be noted that for the basic system, where the pilot is attempting to null  $\phi$  instead of  $\phi_C$ , the miss

distances are substantially reduced. This indicates that the wrong error signal is being controlled by the fire control system. Also, the miss distances for the bombs which were released in a descent are much smaller than those from a level flight condition. This is due to the fact that the time of fall of the bomb is shorter which is directly proportional to the miss distance. It may also be assumed that even larger miss distances may be expected for a bomb which is released in a climb. One other method that may be used to reduce the miss distance is to reduce the release velocity which is directly proportional to the miss distance.

The equations used in this study should be restricted to turning flight where  $\bar{\lambda}$  is not equal to zero. This is the major reason for the large pilot rating for the straight and level trajectory where the system becomes too sensitive. Otherwise, the Cooper-Harper rating for the system indicates that it is a relatively easy task for the pilot. If the straight and level case is disregarded, the data obtained in this study indicates that the pilot is capable of performing the task. This finding is substantiated by the people who have recently flown the General Electric simulator which uses the "Firefly" bombing law.

## Bibliography

1. General Electric Company. Integrated Flight/Fire Control System Phase I Study (F-15), Vol. I. F33615-75-C-3143. Binghamton, New York: GE, July 1977.
2. General Electric Company. Status Report, Firefly II. F33615-75-C-3143. Binghamton, New York: GE, May 1977.
3. Chalk, C.R., et al. Background Information and User Guide for Mil-F-8785B (ASG), "Military Specification - Flying Qualities of Piloted Airplanes." AFFDL-TR-69-72. Wright-Patterson Air Force Base, Ohio: Air Force Flight Dynamics Laboratory, 1969.
4. McRuer, D.T., et al. Human Pilot Dynamics in Compensatory Systems. AFFDL-TR-65-15. Wright-Patterson Air Force Base, Ohio: Research and Technology Division, Air Force Systems Command, July 1965.
5. McRuer, D.T. and H.R. Jex. "A Review of Quasi-Linear Pilot Models." IEEE Transactions on Human Factors in Electronics, HFE-8,3: 231-249 (September 1967).
6. Onstott, E.D., et al. Prediction and Evaluation of Flying Qualities in Turbulence. AFFDL-TR-71-162. Wright-Patterson Air Force Base, Ohio: Air Force Flight Dynamics Laboratory, 1972.
7. Naylor, Flynoy R. Predicting Roll Task Flying Qualities with "Paper Pilot". Unpublished thesis. Wright-Patterson Air Force Base, Ohio: Air Force Institute of Technology, September 1972.
8. McDonnell Douglas Corporation. Technical Description Expo V F-15 Flight Simulator Baseline Configuration. F33615-75-C-1188. St. Louis, Mo: July 1975.
9. Hickey, Herbert J. F-15 Eagle Stability and Control Data for Flying Qualities Analyses. Unpublished Report. Wright-Patterson Air Force Base, Ohio: Aeronautical Systems Division/YFEFF, March 1977.
10. Roskam, Jan. Flight Dynamics of Rigid and Elastic Airplanes. Lawrence, Kansas: Roskam Aviation and Engineering Corporation, 1972.

### Bibliography

11. General Electric Company. Users Manual, Firefly II.  
F33615-75-C-3143. Binghamton, New York: GE, March 1977.
12. School of Mechanical and Aerospace Engineering. User Guide for  
the Frequency Response Analysis Program (FRQRSP).  
F29601-75-C-0121. Stillwater, Oklahoma: Oklahoma State Univer-  
sity, September 1977.

## Appendix A

### Stability Derivatives and Basic Aircraft Data

The following stability derivatives are based upon flight conditions of .6 Mach at 10,000 feet altitude for the F-15 aircraft. These values are for body fixed axes.

$$* \quad C_{y\beta} = - .8595$$

$$** \quad C_{yp} = .1$$

$$** \quad C_{yr} = .32 - .904\alpha_o$$

$$** \quad C_{y\delta_{DT}} = - .086$$

$$* \quad C_{y\delta_r} = .1312$$

$$* \quad C_{l\beta} = - .09741 - .2517\alpha_o$$

$$* \quad C_{lp} = - .24$$

$$** \quad C_{lr} = .048 + 6.66\alpha_o$$

$$* \quad C_{l\delta_A} = .0373$$

$$* \quad C_{l\delta_{DT}} = .04269$$

$$* \quad C_{l\delta_R} = .00327 - .00878\alpha_o$$

\* Derivative obtained from Reference 8 for F-15 aircraft

\*\* Derivative obtained from Reference 9 for YF-15 aircraft

- \*  $C_{m\alpha} = - .2961$
- \*\*  $C_{m\dot{\alpha}} = - 1.2$
- \*  $C_{mq} = - 3.7$
- \*\*  $C_{m\delta_{HT}} = - .688$
- \*  $C_{n\beta} = .1834 - .467\alpha_0$
- \*\*  $C_{np} = - .03$
- \*  $C_{nr} = -.250$
- \*  $C_{n\delta_A} = .00458 - .0416\alpha_0$
- \*  $C_{n\delta_{DT}} = .0229$
- \*  $C_{n\delta_R} = - .086$
- \*  $C_{L\alpha} = 3.782$
- \*  $C_D(\alpha) = .020 - .0905\alpha + 2.325\alpha^2$

Note: These derivatives are only valid for trim angles of attack less than  $8^\circ$ .

Values for  $\alpha_0$  are in radians.

Stability derivatives are non dimensional, therefore, control inputs must be in radians.

The following data was obtained from Reference 8 and represents a typical configuration for the F-15 aircraft.

$$M = 1085, \text{ slugs}$$

$$S = 608, \text{ ft}^2$$

$$b = 42.7, \text{ ft}$$

$$\bar{c} = 16.0, \text{ ft}$$

$$I_x = 25,274, \text{ slugs-ft}^2$$

$$I_y = 155,746, \text{ slugs-ft}^2$$

$$I_z = 175,516, \text{ slugs-ft}^2$$

$$I_{xz} = - 805, \text{ slugs-ft}^2$$

These moments and products of inertia are for body axes.

For the purposes of this report the following values were considered to be constant:

$$\rho/\rho_o = .971$$

$$V_{T_o} = 665, \text{ ft/sec for } .6 \text{ Mach}$$

$$K_B = 2.4 \times 10^{-6} \text{ ft}^{-1} \text{ for low drag MK83}$$

$$g_c = 32.2, \text{ ft/sec}^2$$

$$\bar{q} = 510.5, \text{ lb/ft}^2$$

## Appendix B

### Aircraft Equations of Motion

#### Nonlinear Aircraft Equations

The general force equations of motion for the aircraft are based upon

$$\vec{m}\vec{a} = \frac{m^e d\vec{V}_T}{dt} = m \left( \frac{a^d d\vec{V}_T}{dt} + a^e \vec{\omega} \times \vec{V}_T \right) = \vec{F} \quad (B-1)$$

where  $m$  = Mass of the aircraft

$$\frac{e^d d\vec{V}_T}{dt} = \text{Acceleration in an earth fixed reference frame}$$

$$\begin{aligned} \frac{a^d d\vec{V}_T}{dt} &= \text{Acceleration in an aircraft fixed reference frame} \\ &= \dot{U}\hat{i} + \dot{V}\hat{j} + \dot{W}\hat{k} \end{aligned}$$

$a^e \vec{\omega}$  = Angular velocity of the aircraft reference frame relative to an earth fixed coordinate system

$$= P\hat{i} + Q\hat{j} + R\hat{k}$$

$$\vec{V}_T = U\hat{i} + V\hat{j} + W\hat{k}$$

$$\vec{F} = \vec{F}_A + \vec{F}_B + \vec{F}_T$$

$\vec{F}_A$  = Aerodynamic forces

$$= F_{Ax} \hat{i} + F_{Ay} \hat{j} + F_{Az} \hat{k}$$

It should be noted that  $\hat{i}$ ,  $\hat{j}$ , and  $\hat{k}$  are unit vectors for the body axes of the aircraft. With the aid of the Euler transformation matrix  $[T]$  (see Chapter 2), the body forces,  $\vec{F}_B$ , may be determined as follows:

$$\begin{aligned}\vec{F}_B &= m [T] \begin{bmatrix} 0 & 0 & g_c \end{bmatrix}^T \\ &= -mg_c \sin\theta \hat{i} + mg_c \cos\theta \sin\phi \hat{j} + mg_c \cos\theta \cos\phi \hat{k}\end{aligned}$$

where  $g_c$  is the acceleration coefficient due to gravity.

Also,  $\vec{F}_T$  = Thrust forces

$$= F_{Tx} \hat{i} + F_{Ty} \hat{j} + F_{Tz} \hat{k}$$

$$ae_{\omega}^{\rightarrow} \times \vec{V} = (QW - RV) \hat{i} + (RU - PW) \hat{j} + (PV - QU) \hat{k}$$

Using these definitions, it is possible to write the general force equations of motion as:

$$\dot{U} + QW - RV = -g_c \sin\theta + \frac{F_{Ax}}{m} + \frac{F_{Tx}}{m} \quad (B-2)$$

$$\dot{V} + RU - PW = g_c \cos\theta \sin\phi + \frac{F_{Ay}}{m} + \frac{F_{Ty}}{m} \quad (B-3)$$

$$\dot{W} + PV - QU = g_c \cos\theta \cos\phi + \frac{F_{Az}}{m} + \frac{F_{Tz}}{m} \quad (B-4)$$

(Ref 10:2.24)

The rate of change of the angular momentum, as seen by an observer in inertial space, is equal to vector sum of the external moments. Mathematically this can be written as

$$\frac{e_d \vec{H}}{dt} = \frac{a_d \vec{H}}{dt} + ae_{\omega}^{\rightarrow} \times \vec{H} = \vec{M} \quad (B-5)$$

where  $\vec{H}$  = Angular momentum vector

$$= \begin{bmatrix} \hat{i} & \hat{j} & \hat{k} \end{bmatrix} \begin{bmatrix} I_{xx} & -I_{xy} & -I_{xz} \\ -I_{yz} & I_{yy} & -I_{yz} \\ -I_{zx} & -I_{zy} & I_{zz} \end{bmatrix} \begin{bmatrix} P \\ Q \\ R \end{bmatrix}$$

$\frac{d\vec{H}}{dt}$  = Rate of change of angular momentum in the aircraft reference frame

$$= (I_{xx}\dot{P} - I_{xz}\dot{R}) \hat{i} + (I_{yy}\dot{Q}) \hat{j} + (I_{zz}\dot{R} - I_{zx}\dot{P}) \hat{k}$$

where the xz plane is a plane of symmetry and  $I_{xy} = I_{yx} = I_{yz} = I_{zy} = 0$ .

$$\vec{\omega} \times \vec{H} = \left[ -I_{xz} PQ + (I_{zz} - I_{yy}) QR \right] \hat{i} + \left[ (I_{xx} - I_{zz}) PR + I_{xz} (P^2 - R^2) \right] \hat{j} + \left[ I_{xz} QR + (I_{yy} - I_{xx}) PQ \right] \hat{k}$$

$$\vec{M} = \vec{M}_A + \vec{M}_T$$

$$\vec{M}_A = L_A \hat{i} + M_A \hat{j} + N_A \hat{k}$$

$$\vec{M}_T = L_T \hat{i} + M_T \hat{j} + N_T \hat{k}$$

Combining the above equations yields:

$$I_{xx}\dot{P} - I_{xz}\dot{R} - I_{xz} PQ + (I_{zz} - I_{yy}) QR = L_A + L_T \quad (B-6)$$

$$I_{yy}\dot{Q} + (I_{xx} - I_{zz}) PR + I_{xz} (P^2 - R^2) = M_A + M_T \quad (B-7)$$

$$I_{zz}\dot{R} - I_{xz}\dot{P} + (I_{yy} - I_{xx}) PQ + I_{xz} QR = N_A + N_T \quad (B-8)$$

(Ref 10:2.10)

These six equations of motion (equations B-2 thru B-4 and B-6 thru B-8) contain eight unknowns which are: U, V, W, P, Q, R,  $\theta$ ,  $\phi$ . To correct this problem, the three kinematic equations may be derived with the aid of the Euler transformation matrices (see Chapter 2).

$$ae_{\omega} = \begin{bmatrix} P \\ Q \\ R \end{bmatrix} = \begin{bmatrix} \phi \end{bmatrix} \begin{bmatrix} \theta \end{bmatrix} \begin{bmatrix} \psi \end{bmatrix} \begin{bmatrix} 0 \\ 0 \\ \dot{\psi} \end{bmatrix} + \begin{bmatrix} \phi \end{bmatrix} \begin{bmatrix} \theta \end{bmatrix} \begin{bmatrix} 0 \\ \dot{\theta} \\ 0 \end{bmatrix} + \begin{bmatrix} \phi \end{bmatrix} \begin{bmatrix} \dot{\phi} \\ 0 \\ 0 \end{bmatrix}$$

$$= \begin{bmatrix} 1 & 0 & -\sin\theta \\ 0 & \cos\phi & \cos\theta\sin\phi \\ 0 & -\sin\phi & \cos\theta\cos\phi \end{bmatrix} \begin{bmatrix} \dot{\phi} \\ \dot{\theta} \\ \dot{\psi} \end{bmatrix}$$

Solving the above linear set of equations for  $\dot{\phi}$ ,  $\dot{\theta}$ , and  $\dot{\psi}$  yields:

$$\dot{\phi} = P + Q \sin\phi \tan\theta + R \cos\phi \tan\theta \quad (B-9)$$

$$\dot{\theta} = Q \cos\phi - R \sin\phi \quad (B-10)$$

$$\dot{\psi} = (Q \sin\phi + R \cos\phi)/\cos\theta \quad (B-11)$$

(Ref 10:2.22)

In the development of the previous equations, the following assumptions apply:

The earth fixed coordinates are considered to be inertial coordinates.

The aircraft coordinate system is body fixed with the origin at the center of gravity.

The mass of the aircraft is constant.

The angular momentum due to spinning rotors has been neglected.

The xz plane is a plane of symmetry.

The aircraft is a rigid body.

In order to solve these nine aircraft equations of motion, it is necessary that  $U_o$ ,  $V_o$ ,  $W_o$ ,  $P_o$ ,  $Q_o$ ,  $R_o$ ,  $\theta_o$ , and  $\phi_o$  be known. From the geometry equations (see Chapter two), values for  $\alpha_o$ ,  $\phi_o$ , and  $\theta_o$  were determined by solving for the required trajectory of the aircraft.

Knowing  $\alpha_o$ ,  $U_o$  and  $W_o$  can be obtained from

$$U_o = V_{T_o} \cos \alpha_o \quad (B-12)$$

$$W_o = V_{T_o} \sin \alpha_o \quad (B-13)$$

Also for coordinated flight with zero sideslip,  $V_o = F_{A_y} = 0$ .

Equations B-2 through B-4 and B-6 through B-10 may be used to solve the remaining eight unknowns ( $P_o$ ,  $Q_o$ ,  $R_o$ ,  $F_{A_x}$ ,  $F_{A_z}$ ,  $L_A$ ,  $M_A$ ,  $N_A$ ) for steady state flight conditions.  $P$ ,  $Q$ ,  $R$  can be obtained from equations B-3, B-9 and B-10 as follows:

$$Q_o = R_o \tan \phi_o \quad (B-14)$$

$$P_o = - R_o (\tan \phi_o \sin \phi_o \tan \theta_o + \cos \phi_o \tan \theta_o) \quad (B-15)$$

$$R_o = \frac{g_c \sin \phi_o \cos \theta_o}{U_o + W_o (\tan \phi_o \sin \phi_o \tan \theta_o + \cos \phi_o \tan \theta_o)} \quad (B-16)$$

### Linear Aircraft Equations

These nine, coupled, nonlinear, differential equations describe the general motion of the aircraft. Since this study is interested in the aircraft dynamic frequency response about some equilibrium state, the perturbation technique is appropriate. Using this approach, the equations may be linearized and Laplace transformations used to study the frequency response. This can be accomplished by:

- (1) Considering the eight state variables ( $U$ ,  $V$ ,  $W$ ,  $P$ ,  $Q$ ,  $R$ ,

$\theta, \phi$ ) as being composed of some equilibrium (steady state) value and some perturbation value. These variables can then be written as:

$$\begin{aligned} U &= U_o + u & P &= P_o + p & \theta &= \theta_o + \theta \\ V &= V_o + v & Q &= Q_o + q & \phi &= \phi_o + \phi \\ W &= W_o + w & R &= R_o + r \end{aligned}$$

The thrust and aerodynamic forces and moments may be expressed as:

$$\begin{aligned} F_{A_x} &= F_{A_{x_o}} + f_{A_x} & F_{T_x} &= F_{T_{x_o}} + f_{T_x} \\ F_{A_y} &= F_{A_{y_o}} + f_{A_y} & F_{T_y} &= F_{T_{y_o}} + f_{T_y} \\ F_{A_z} &= F_{A_{z_o}} + f_{A_z} & F_{T_z} &= F_{T_{z_o}} + f_{T_z} \\ L_A &= L_{A_o} + l_A & L_T &= L_{T_o} + l_T \\ M_A &= M_{A_o} + m_A & M_T &= M_{T_o} + m_T \\ N_A &= N_{A_o} + n_A & N_T &= N_{T_o} + n_T \end{aligned}$$

Where the steady state values are denoted by the subscript (o) and the perturbed state quantity is represented by lower case symbol.

(2) Defining the perturbation angles  $\phi$  and  $\theta$  such that:

$$\begin{aligned} \cos \theta &\approx 1 & \cos \phi &\approx 1 \\ \sin \theta &\approx \theta & \sin \phi &\approx \phi \end{aligned}$$

In general, this relationship holds for angles less than  $15^\circ$ .

(Ref 10:2.33)

(3) Assuming that all products and cross products of the perturbation variables may be neglected when compared to the magnitude of the perturbations themselves or by using the linear terms of a Taylor series expansion about the nominal conditions.

(4) Noting that the steady state equations of motion and kinematic equations which are embedded in the perturbed state equations have already been satisfied and therefore can be eliminated (Ref 10:2.33).

With these basic assumptions, the linearized force equations are:

$$\dot{u} - V_0 r - R_0 v + W_0 q + Q_0 w = -g_c \theta \cos \theta_0 + \frac{f_{A_x}}{m} + \frac{f_{T_x}}{m} \quad (B-17)$$

$$\begin{aligned} \dot{v} + U_0 r + R_0 u - W_0 p - P_0 w = & -g_c \theta \sin \theta_0 \sin \phi_0 + \\ & g_c \phi \cos \theta_0 \cos \phi_0 + \frac{f_{A_y}}{m} + \frac{f_{T_y}}{m} \end{aligned} \quad (B-18)$$

$$\begin{aligned} \dot{w} - U_0 q - Q_0 u + V_0 p + P_0 v = & -g_c \theta \sin \theta_0 \cos \phi_0 - \\ & g_c \phi \cos \theta_0 \sin \phi_0 + \frac{f_{A_z}}{m} + \frac{f_{T_z}}{m} \end{aligned} \quad (B-19)$$

(Ref 10:2.33)

For this analysis, the perturbations due to thrust are assumed to be small and have been neglected. Also, for normal flight conditions, the aircraft is assumed to be flying a trajectory that will result in a reliable release without any inputs to the controls. This assumes the aircraft is in coordinated flight where  $V_0$  is zero.

The value  $\frac{f_{A_x}}{m}$  may be determined from the following equation:

$$F_{A_x} = C_x \bar{q} S \quad (B-20)$$

where,  $C_x = C_L(\bar{\alpha}) \sin \bar{\alpha} - C_D(\bar{\alpha}) \cos \bar{\alpha} = 3.782\bar{\alpha} \sin \bar{\alpha} - (.020 - .0905\bar{\alpha} + 2.325\bar{\alpha}^2) \cos \bar{\alpha}$  (Ref 8 :19,20)

This equation may be linearized by using the Taylor's series expansion limited to linear terms where:

$$f_{A_x} = \left. \frac{\partial F_{A_x}}{\partial \left(\frac{u}{U_o}\right)} \right|_o \left(\frac{u}{U_o}\right) + \left. \frac{\partial F_{A_x}}{\partial \bar{\alpha}} \right|_o \alpha$$

where,  $\left. \frac{\partial F_{A_x}}{\partial \left(\frac{u}{U_o}\right)} \right|_o = \bar{q} S \frac{\partial C_x}{\partial \left(\frac{u}{U_o}\right)} + C_x S \frac{\partial \bar{q}}{\partial \left(\frac{u}{U_o}\right)}$   
 $= 2 \bar{q} S C_x$

$$\left. \frac{\partial F_{A_x}}{\partial \bar{\alpha}} \right|_o = \bar{q} S \left. \frac{\partial C_x}{\partial \alpha} \right|_o$$

$$\frac{f_{A_x}}{m} = \frac{2 \bar{q} S u}{m U_o} (3.782\alpha_o \sin \alpha_o - .020 \cos \alpha_o + .0905\alpha_o \cos \alpha_o -$$

$$2.325\alpha_o^2 \cos \alpha_o) + \frac{\bar{q} S \alpha}{m} (3.782 \sin \alpha_o + 3.782\alpha_o \cos \alpha_o +$$

$$.020 \sin \alpha_o + .0905 \cos \alpha_o - .0905\alpha_o \sin \alpha_o - 4.65\alpha_o \cos \alpha_o +$$

$$2.325\alpha_o^2 \sin \alpha_o) \quad (B-21)$$

Combining like terms and using the flight conditions referenced in appendix A,  $\frac{f_{A_x}}{m}$  may be written as:

$$\frac{f_{A_x}}{m} = u \left[ .86 (3.782\alpha_o \sin \alpha_o - .020 \cos \alpha_o + .0905\alpha_o \cos \alpha_o -$$

$$2.325\alpha_0^2 \cos\alpha_0) + \alpha [286 (3.802 \sin\alpha_0 - .8680\alpha_0 \cos\alpha_0 + .0905 \cos\alpha_0 - .0905\alpha_0 \sin\alpha_0 + 2.325\alpha_0^2 \sin\alpha_0)] \quad (B-22)$$

The value for  $\frac{f_{A_z}}{m}$  may be determined using the same method.

$$F_{A_z} = C_z \bar{q} S \quad (B-23)$$

where,  $C_z = -C_L(\bar{\alpha}) \cos \bar{\alpha} - C_D(\bar{\alpha}) \sin \bar{\alpha}$

$$= -3.782\bar{\alpha} \cos\bar{\alpha} - (.020 - .0905\bar{\alpha} + 2.325\bar{\alpha}^2) \sin\bar{\alpha}$$

Using the Taylor's series expansion,

$$\begin{aligned} \frac{f_{A_z}}{m} &= \left. \frac{\partial F_{A_z}}{\partial \left(\frac{u}{U}\right)} \right|_0 \left(\frac{u}{U}\right) + \left. \frac{\partial F_{A_z}}{\partial \bar{\alpha}} \right|_0 \alpha \\ &= 2 \bar{q} S C_z \frac{u}{U_0} + \bar{q} S \left. \frac{\partial C_z}{\partial \alpha} \right|_0 \alpha \\ \frac{f_{A_z}}{m} &= u \left[ .86(-3.782\alpha_0 \cos\alpha_0 - .020 \sin\alpha_0 + .0905\alpha_0 \sin\alpha_0 - 2.325\alpha_0^2 \sin\alpha_0) \right] \\ &+ \alpha \left[ 286(-3.802 \cos\alpha_0 - .868\alpha_0 \sin\alpha_0 + .0905\alpha_0 \cos\alpha_0 + .0905 \sin\alpha_0 - 2.325\alpha_0^2 \cos\alpha_0) \right] \quad (B-24) \end{aligned}$$

$\frac{f_{A_y}}{m}$  may be determined from:

$$\frac{f_{A_y}}{m} = \frac{\bar{q} S}{m} \left( C_{y\beta} \beta + C_{yp} \frac{pb}{2U_0} + C_{yr} \frac{rb}{2U_0} + C_{y\delta_{DT}} \delta_{DT} + C_{y\delta_R} \delta_R \right) \quad (B-25)$$

(Ref 10:4.113)

$$= 286. \left[ -.8595\beta + .00321p + (.0103 - .029\alpha_0)r - .086 \delta_{DT} + .1312 \delta_R \right] \quad (B-26)$$

Combining equations B-17 and B-22, B-18 and B-24, and B-19 and B-26 and also collecting like terms yields:

$$\begin{aligned}
 & u \left[ .86 (3.782\alpha_0 \sin\alpha_0 - .020 \cos\alpha_0 + .0905\alpha_0 \cos\alpha_0 - 2.325\alpha_0^2 \cos\alpha_0) - \right. \\
 & \left. s \right] + \beta(665 R_0) + \alpha \left[ 286(3.802 \sin\alpha_0 - .868\alpha_0 \cos\alpha_0 + .0905 \cos\alpha_0 - \right. \\
 & \left. .0905\alpha_0 \sin\alpha_0 + 2.325\alpha_0^2 \sin\alpha_0) - 665 Q_0 \right] - q (W_0) - \\
 & \theta (32.2 \cos\theta_0) = 0 \qquad \qquad \qquad (B-27)
 \end{aligned}$$

$$\begin{aligned}
 & - u (R_0) - \beta(245.8 + 665s) + \alpha(665P_0) + p (W_0 + .918) + r (2.946 - \\
 & 8.249\alpha_0 - U_0) - \theta (32.2 \sin\theta_0 \sin\phi_0) + \phi(32.2 \cos\theta_0 \cos\phi_0) - \\
 & \delta_{DT} (24.6) + \delta_R (37.52) = 0 \qquad \qquad \qquad (B-28)
 \end{aligned}$$

$$\begin{aligned}
 & u \left[ Q_0 + .86 (- 3.782\alpha_0 \cos\alpha_0 - .020 \sin\alpha_0 + .0905\alpha_0 \sin\alpha_0 - \right. \\
 & \left. 2.325\alpha_0^2 \sin\alpha_0) \right] - \beta(665P_0) + \alpha \left[ 286 (- 3.802 \cos\alpha_0 - .868\alpha_0 \sin\alpha_0 + \right. \\
 & \left. .0905\alpha_0 \cos\alpha_0 + .0905 \sin\alpha_0 - 2.325\alpha_0^2 \cos\alpha_0) - 665s \right] + q (U_0) - \\
 & \theta (32.2 \sin\theta_0 \cos\phi_0) - \phi (32.2 \cos\theta_0 \sin\phi_0) = 0 \qquad \qquad \qquad (B-29)
 \end{aligned}$$

It should be noted that in the preceeding equations  $V_0$  is equal to zero and  $s$  represents the Laplace transform variable.

The linearized moment equations may be written as:

$$I_x \dot{p} - I_{xz} \dot{r} - I_{xz} (P_0 q + Q_0 p) + (I_z - I_y) (R_0 q + Q_0 r) = m_A + m_T \qquad (B-30)$$

$$I_y \dot{q} + (I_x - I_z) (P_0 r + R_0 p) + I_{xz} (2 P_0 p - 2 R_0 r) = m_A + m_T \qquad (B-31)$$

$$I_z \dot{r} - I_{xz} \dot{p} + (I_y - I_x) (P_o q + Q_o p) + I_{xz} (Q_o r + R_o q) = n_A + n_T \quad (B-32)$$

(Ref 10 :2.33)

The same assumptions apply here as in the force equations, that is, the perturbations due to thrust are assumed to be small and  $V_o = 0$ . The perturbed rolling moment may be written as:

$$l_A = \bar{q} S b \left( C_{l\beta} \beta + C_{lp} \frac{pb}{2U_o} + C_{lr} \frac{rb}{2U_o} + C_{l\delta A} \delta_A + C_{l\delta DT} \delta_{DT} + C_{l\delta R} \delta_R \right) \quad (B-33)$$

(Ref 10 :4.113)

Again, using the flight conditions from appendix A:

$$l_A = 13.25 \times 10^6 \left[ (-.09741 - .2517\alpha_o) \beta - .0077 p + (.00154 + .2138\alpha_o) r + .0373 \delta_A + .0427 \delta_{DT} + (.00327 - .00878\alpha_o) \delta_R \right] \quad (B-34)$$

The perturbed pitching moment may be determined as follows:

$$m_A = \bar{q} S \bar{c} \left( C_{m_u} \frac{u}{U_o} + C_{m\alpha} \alpha + C_{m\dot{\alpha}} \frac{\dot{\alpha}\bar{c}}{2U_o} + C_{m_q} \frac{q\bar{c}}{2U_o} + C_{m\delta HT} \delta_{HT} \right) \quad (B-35)$$

(Ref 10 :4.113)

where  $C_{m_u}$  is negligible for mach numbers below the transonic range.

$$m_A = 4.96 \times 10^6 (-.2961\alpha - .0144\dot{\alpha} - .0445q - .688 \delta_{HT}) \quad (B-36)$$

The perturbed yawing moment is:

$$n_A = \bar{q} S b \left( C_{n\beta} \beta + C_{np} \frac{pb}{2U_o} + C_{nr} \frac{rb}{2U_o} + C_{n\delta A} \delta_A + C_{n\delta DT} \delta_{DT} + C_{n\delta R} \delta_R \right) \quad (B-37)$$

$$\eta_A = 13.25 \times 10^6 \left[ (.1834 - .467\alpha_o)_\beta - .000963 p - .0080 r + \right. \\ \left. (.00458 - .0416\alpha_o) \delta_A + .0229 \delta_{DT} - .086 \delta_R \right] \quad (B-38)$$

After combining the terms for each variable, and dividing through by  $10^6$ , the three angular momentum equations are:

$$-\beta (1.29 + 3.335\alpha_o) - p (.102 + .0253s + .0008 Q_o) - q (.0008P_o + \\ .0197 R_o) + r (.0204 + 2.833\alpha_o - .0008s - .0197 Q_o) + \delta_A (.494) + \\ \delta_{DT} (.5656) + \delta_R (.0433 - .116\alpha_o) = 0 \quad (B-39)$$

$$-\alpha (1.47 + .0717s) + p (.0016 P_o + .150 R_o) - q (.221 + .1557s) + \\ r (.150 P_o - .0016 R_o) - \delta_{HT} (3.416) = 0 \quad (B-40)$$

$$\beta (2.43 - 6.187\alpha_o) - p (.01276 + .0008s + .130 Q_o) + q (-.130 P_o + \\ .0008 R_o) + r (-.1063 - .1755s + .0008 Q_o) + \delta_A (.0607 - \\ .551\alpha_o) + \delta_{DT} (.303) - \delta_R (1.14) = 0 \quad (B-41)$$

The three linearized kinematic equations are:

$$q \frac{\sin\phi_o}{\cos\theta_o} + r \frac{\cos\phi_o}{\cos\theta_o} - \psi s + \theta \left[ \frac{\tan\theta_o}{\cos\theta_o} (Q_o \sin\phi_o + R_o \cos\phi_o) \right] + \\ \phi \left( Q_o \frac{\cos\phi_o}{\cos\theta_o} - R_o \frac{\sin\phi_o}{\cos\theta_o} \right) = 0 \quad (B-42)$$

$$q (\cos\phi_o) - r (\sin\phi_o) - \theta s - \phi (Q_o \sin\phi_o + R_o \cos\phi_o) = 0 \quad (B-43)$$

$$p + q (\sin\phi_o \tan\theta_o) + r (\cos\phi_o \tan\theta_o) + \theta \left( Q_o \frac{\sin\phi_o}{\cos^2\theta_o} + \right.$$

$$\left. R_o \frac{\cos\phi_o}{\cos^2\theta_o} \right) + \phi (Q_o \cos\phi_o \tan\theta_o - R_o \sin\phi_o \tan\theta_o - s) = 0 \quad (\text{B-44})$$

The nine linearized aircraft equations are summarized in Table XI.

Table XI

## Summary of Linearized Aircraft Equations

Force equations:

$$u \left[ .86(3.782\alpha_0 \sin\alpha_0 - .020\cos\alpha_0 + .0905\alpha_0 \cos\alpha_0 - 2.325\alpha_0^2 \cos\alpha_0) - s \right] + \beta(665R_0) + \alpha \left[ 286(3.802\sin\alpha_0 - .868\alpha_0 \cos\alpha_0 + .0905\cos\alpha_0 - .0905\alpha_0 \sin\alpha_0 + 2.325\alpha_0^2 \sin\alpha_0) - 665Q_0 \right] - q(W_0) - \theta(32.2\cos\theta_0) = 0$$

$$-u(R_0) - \theta(245.8 + 665s) + \alpha(665P_0) + p(W_0 + 918) + r(2.946 - 8.249\alpha_0 - U_0) - \theta(32.2\sin\theta_0 \sin\phi_0) + \phi(32.2\cos\theta_0 \cos\phi_0) -$$

$$\delta_{DT}(24.6) + \delta_R(37.52) = 0$$

$$u \left[ Q_0 + .86(-3.782\alpha_0 \cos\alpha_0 - .020\sin\alpha_0 + .0905\alpha_0 \sin\alpha_0 - 2.325\alpha_0^2 \sin\alpha_0) \right] - \beta(665P_0) + \alpha \left[ 286(-3.802\cos\alpha_0 -$$

$$.868\alpha_0 \sin\alpha_0 + .0905\alpha_0 \cos\alpha_0 + .0905\sin\alpha_0 - 2.325\alpha_0^2 \cos\alpha_0) - 665s \right] + q(U_0) - \theta(32.2\sin\theta_0 \cos\phi_0) -$$

$$\phi(32.2\cos\theta_0 \sin\phi_0) = 0$$

Moment equations:

$$-\beta(1.29 + 3.335\alpha_0) - p(.102 + .0253s + .0008Q_0) - q(.0008P_0 + .0197R_0) + r(.0204 + 2.833\alpha_0 - .0008s - .0197Q_0) +$$

$$\delta_A(.494) + \delta_{DT}(.5656) + \delta_R(.0433 - .116\alpha_0) = 0$$

AD-A048 882

AIR FORCE INST OF TECH WRIGHT-PATTERSON AFB OHIO SCH--ETC F/G 15/7  
A FEASIBILITY STUDY OF A MANUAL BOMB RELEASE WHILE IN A TURN. (U)

DEC 77 J D WALTON

AFIT/OAE/AA/77D-17

UNCLASSIFIED

NL

2 OF 2

AD  
A048882



END  
DATE  
FILMED

2-78

DDC

Table XI (Continued)

Summary of Linearized Aircraft Equations

$$-\alpha(1.47+.0717s)+p(.0016P_o+.150R_o-q(.221+.1557s)+r(.150P_o-.0016R_o)-\delta_{HT}(3.416) = 0$$

$$\beta(2.43-6.187\alpha_o)-p(.01276+.0008s+.130Q_o)+q(-.130P_o+.0008R_o)+r(-.1063-.1755s+.0008Q_o)+\delta_A(.0607-.551\alpha_o)+$$

$$\delta_{DT}(.303)-\delta_R(1.14) = 0$$

Kinematic equations:

$$q\left(\frac{\sin\phi_o}{\cos\theta_o}\right)+r\left(\frac{\cos\phi_o}{\cos\theta_o}\right)-\psi s+\theta\left[\frac{\tan\theta_o}{\cos\theta_o}(Q_o\sin\phi_o+R_o\cos\phi_o)\right]+\phi\left(Q_o\frac{\cos\phi_o}{\cos\theta_o}-R_o\frac{\sin\phi_o}{\cos\theta_o}\right) = 0$$

$$q(\cos\phi_o)-r(\sin\phi_o)-\theta s-\phi(Q_o\sin\phi_o+R_o\cos\phi_o) = 0$$

$$p+q(\sin\phi_o\tan\theta_o)+r(\cos\phi_o\tan\theta_o)+\theta\left[Q_o\left(\frac{\sin\phi_o}{\cos^2\theta_o}\right)+R_o\left(\frac{\cos\phi_o}{\cos^2\theta_o}\right)\right]+\phi\left(Q_o\cos\phi_o\tan\theta_o-R_o\sin\phi_o\tan\theta_o-s\right) = 0$$

## Appendix C

### Flight Control Equations

Since this study is based upon the frequency response of the aircraft, linearized flight control equations must be included in the system model. The F-15 flight control system is basically linear with only a few appropriately placed limiters, deadbands and gain schedulers. Because this study is an examination of the dynamic response about some nominal flight condition, most of these nonlinearities can be either avoided, neglected or linearized.

The actuators for the control surfaces are depicted in figures 11 through 14 (Ref 11 :25,26). Since these actuators are capable of responses of up to 20 radians per second, they have not been included in this analysis. The reason for this is the primary frequency range of interest is below ten radians per second. The simplified block diagrams for the pitch, roll and yaw axis are presented in figures 15 , 16 , and 17 (Ref 11:29-32). It should be noted that all the inputs are in pounds force and all the control displacements are in radians.

#### F-15 Flight Controls

With these assumptions and clarifications, the primary pitch axis control laws may be written as:

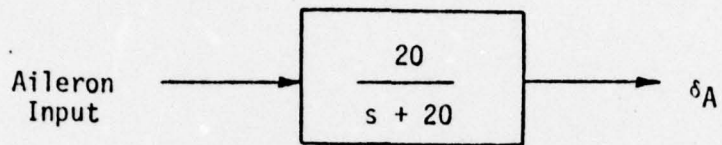


Fig. 11. Aileron Actuator

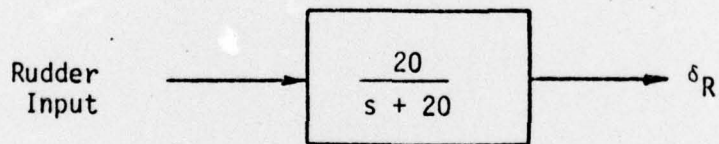


Fig. 12. Rudder Actuator

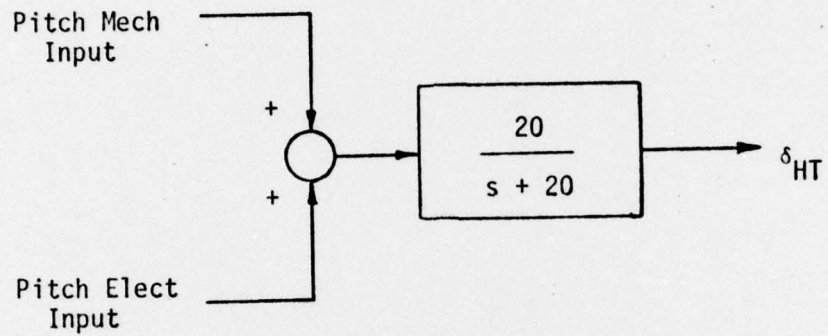


Fig. 13. Horizontal Tail Actuator

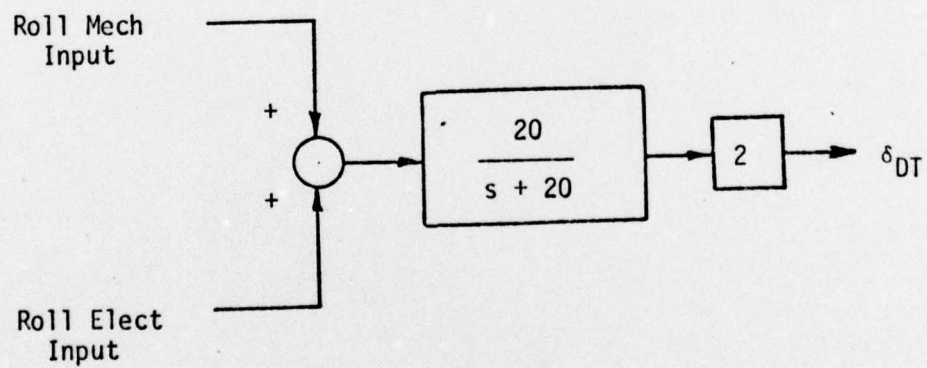


Fig. 14. Differential Tail Actuator

$$\text{Pitch Elec Input} = \left\{ - \left[ F_{ES} \left( \frac{1}{3.73} \right) \left( \frac{5}{5+s} \right) \right] + \left[ \frac{F_{Az}}{mg_c} + q (12.42) \left( \frac{3s}{3s+1} \right) + s q (.68) \right] \left( \frac{30+3s}{30+s} \right) \right\} \cdot 1.5 \left( \frac{1}{s} \right) \left( \frac{1}{57.3} \right) \quad (C-1)$$

$$\text{Pitch Mech Input} = \left\{ \left[ -F_{ES} (.1)(2) - \frac{F_z}{mg_c} + q s (.5) \right] \frac{1}{3.75} + \left\{ - \left[ F_{ES} \left( \frac{1}{3.73} \right) \left( \frac{5}{5+s} \right) \right] + \left[ \frac{F_{Az}}{mg_c} + q (12.42) \left( \frac{3s}{3s+1} \right) + s q (.68) \right] \left( \frac{30+3s}{30+s} \right) \right\} 1.5 \left( \frac{1}{s} \right) (.2) \right\} \frac{1.5}{s} - F_{ES} (.1)(.6464)(2) \left\} \frac{1}{57.3} \quad (C-2)$$

From Fig 13, it can be seen that:

$$\text{Pitch Elec Input} + \text{Pitch Mech Input} = \delta_{HT} \quad (C-3)$$

$$\delta_{HT} = -F_{ES} \left( \frac{.0023s^3 + .048s^2 + .0526s + .0105}{s^3 + 5s^2} \right) + \frac{F_{Az}}{mg_c} \left( \frac{.0786s^3 + .8816s^2 + .835s + .2356}{s^3 + 30s^2} \right) + q \left( \frac{.1603s^4 + 4.798s^3 + 36.14s^2 + 40.24s + 8.94}{3s^3 + 91s^2 + 30s} \right) \quad (C-4)$$

$$\text{where } \frac{F_{Az}}{mg_c} = u \left[ .0267(-3.782\alpha_o \cos\alpha_o - .020\sin\alpha_o + .0905\alpha_o \sin\alpha_o - 2.325\alpha_o^2 \sin\alpha_o) \right] + \alpha \left[ 8.885(-3.802\cos\alpha_o - .868\alpha_o \sin\alpha_o + .0905\alpha_o \cos\alpha_o + .0905\sin\alpha_o - 2.325\alpha_o^2 \cos\alpha_o) \right] \quad (C-5)$$

From Fig. 16, the roll axis flight control equations are:

$$F_{AS} = 23.87 \delta_A \quad (C-6)$$

$$\left[ F_{AS} \left( \frac{1}{1+.3s} \right) \left( \frac{1}{57.3} \right) - p \right] (.0625) = \delta_{DT_{ELEC}} \quad (C-7)$$

$$F_{AS} (.24) (10) \left( \frac{1}{57.3} \right) \left( \frac{.3}{2} \right) = \delta_{DT_{MECH}} \quad (C-8)$$

The two differential tail inputs ( $\delta_{DT_{ELEC}}$  and  $\delta_{DT_{MECH}}$ ) may be summed together to obtain the differential tail displacement (see Fig. 14 ).

$$\delta_{DT_{ELEC}} + \delta_{DT_{MECH}} = 2 \delta_{DT} \quad (C-9)$$

$$F_{AS} \left( \frac{.0019s + .0074}{3s + 1} \right) - .0625p = 2 \delta_{DT} \quad (C-10)$$

The primary yaw axis flight control equation can be obtained from Fig. 17 .

$$F_{RP} (.5) \left( \frac{1}{57.3} \right) \left( \frac{10}{10+s} \right) + \left[ \frac{F_{Ay}}{m} (.00537) + r \left( \frac{2s}{2s+1} \right)^2 - (\alpha P_o + p \alpha_o) \left( \frac{s}{s+1} \right) \right] \cdot \left( \frac{s+.5}{s} \right) (.84) + F_{RP} (.5) \frac{1}{57.3} = \delta_R \quad (C-11)$$

$$\text{where } \frac{F_{Ay}}{m} = 286 \left[ -.8595\beta + .00321p + (.0103 - .029\alpha_o) r - .086 \delta_{DT} + .1312 \delta_R \right] \quad (C-12)$$

$$F_{RP} \left( \frac{.0087s + .174}{s + 10} \right) = \beta \left( \frac{1.109s + .555}{s} \right) + \alpha \left( \frac{.84P_o s + .42P_o}{s + 1} \right) +$$

$$\begin{aligned}
& p \left( \frac{(.84\alpha_o - .0041) s^2 + (.42\alpha_o - .0062)s - .0021}{s^2 + s} \right) + \\
& r \left( \frac{(.15\alpha_o - 3.4)s^3 + (.22\alpha_o - 1.76)s^2 + (.11\alpha_o - .04)s + .019\alpha_o - .0066}{4s^3 + 4s^2 + s} \right) + \\
& \delta_{DT} \left( \frac{.1107s + .0553}{s} \right) + \delta_R \left( \frac{.8307s - .0845}{s} \right) \quad (C-13)
\end{aligned}$$

### Firefly Flight Controls

The "Firefly" automated system has been studied, in order to have a baseline with which to compare the manually operated system. Figures 18, 19, and 20 depict the F-15 flight control laws which have been modified for the Firefly configuration. Referring to Fig. 18, the augmented pitch axis flight control equation may be written as:

$$\begin{aligned}
\text{Pitch Elect Input} = & \left[ -F_{ES} \left( \frac{1}{3.73} \right) \left( \frac{32.2}{665} \right) \left( \frac{5}{5+s} \right) + q \left( \frac{30+3s}{30+s} \right) \right] \cdot \\
& \left[ \left( \frac{322}{510} \right) \left( 1 + \frac{3}{s} \right) \left( \frac{1}{57.3} \right) \right] \quad (C-14)
\end{aligned}$$

$$\begin{aligned}
\text{Pitch Mech Input} = & \left\{ \left[ -F_{ES} (.1)(2) - \frac{F_z}{mg_c} + q s (.5) \right] \frac{1}{3.75} + \right. \\
& \left\{ - \left[ F_{ES} \left( \frac{1}{3.73} \right) \left( \frac{5}{5+s} \right) \right] + \left[ \frac{F_{Az}}{mg_c} + q (12.42) \left( \frac{3s}{3s+1} \right) + \right. \right. \quad (C-2) \\
& \left. \left. s q (.68) \right] \left[ \frac{30+3s}{30+s} \right] \right\} 1.5 \left( \frac{1}{s} \right) (.2) \frac{1.5}{s} - F_{ES} (.1)(.6464)(2) \left. \right\} \frac{1}{57.3}
\end{aligned}$$

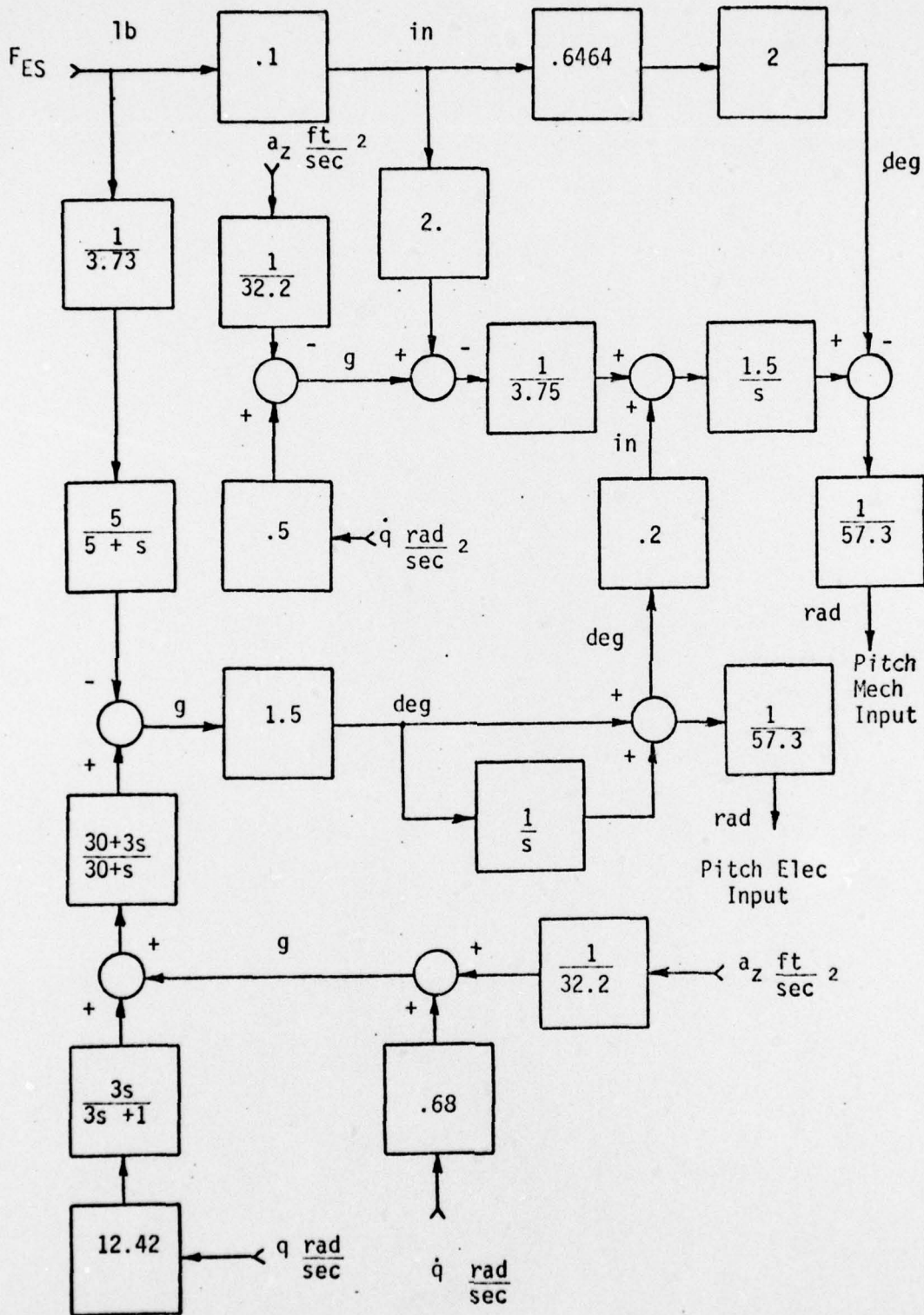


Fig. 15. Primary Pitch Axis Control Laws (F-15)

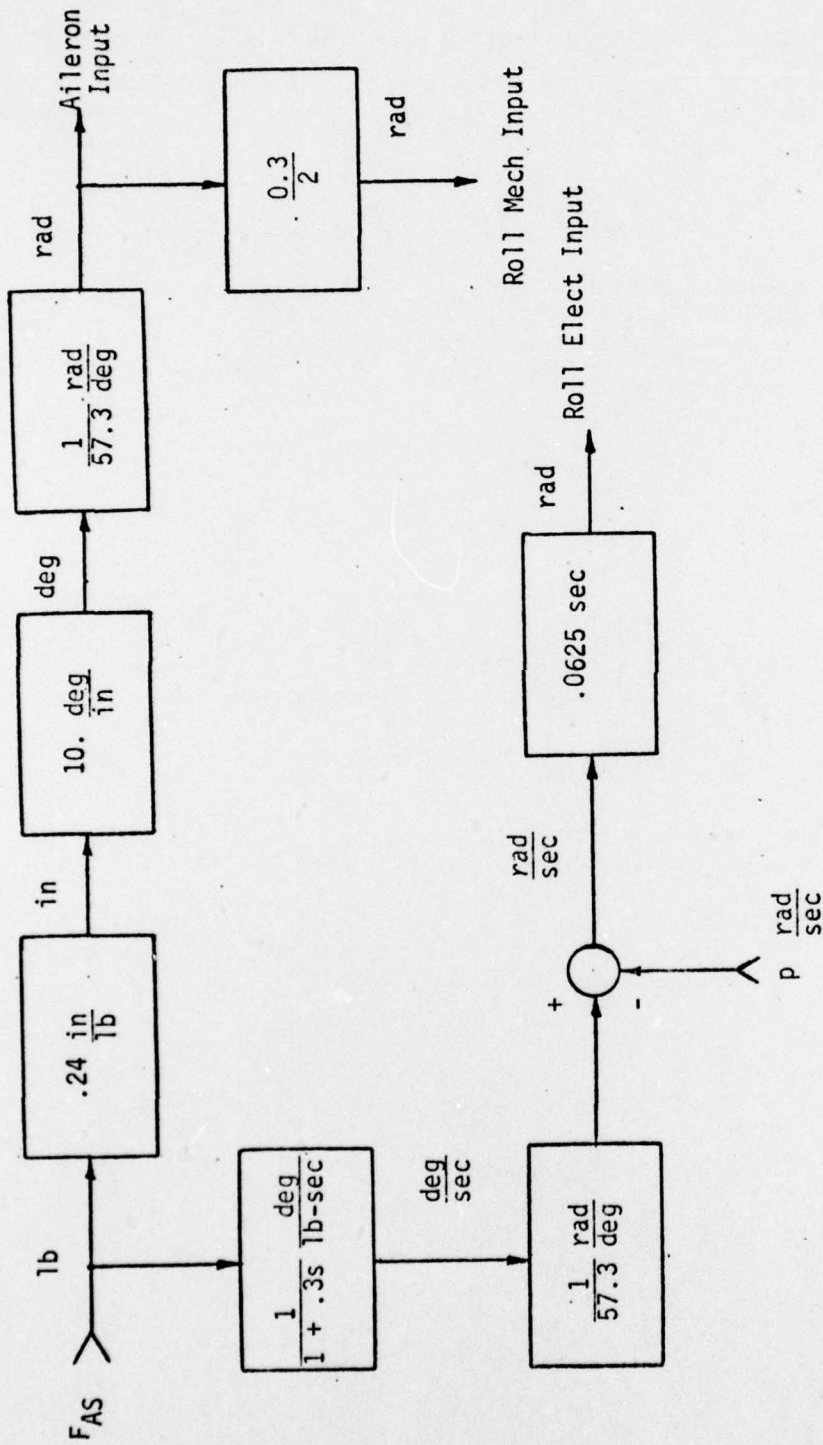


Fig. 16. Primary Roll Axis Control Laws (F-15)

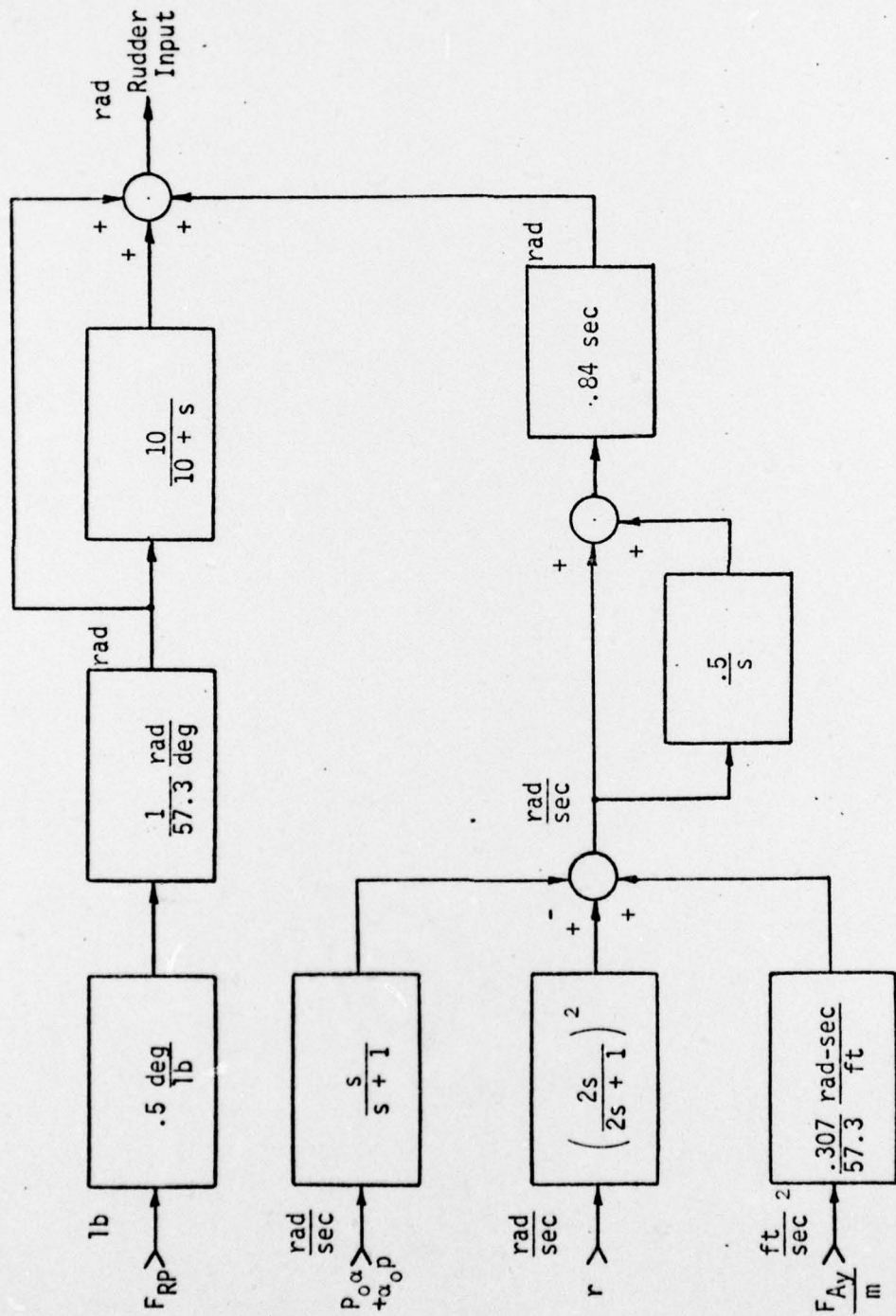


Fig. 17. Primary Yaw Axis Control Laws (F-15)

By summing the electrical input and the mechanical input, the pitch axis equation for the flight control is:

$$\delta_{HT} = -F_{ES} \left( \frac{.0023s^3 + .0136s^2 + .0196s + .0105}{5s^2 + s^3} \right) + \frac{F_{AZ}}{mg_C} \left( \frac{.0166s^2 + .049s + .2356}{30s^2 + s^3} \right) + q \left( \frac{.158s^3 + 3.06s^2 + 13.82s + 9.94}{3s^3 + 91s^2 + 30s} \right) \quad (C-15)$$

For the aileron input there is no change from the basic F-15 flight control system. Therefore:

$$F_{AS} = 23.87 \delta_A \quad (C-16)$$

However, the output from the fire control equation,  $p_C$ , is fed into the roll axis of the differential tail. Figure 19 shows the  $p_C$  input plus the slight change in flight control configuration. This diagram leads to the following equations:

$$\text{Roll Elect Input} = \left[ F_{AS} \left( \frac{1}{1+.3s} \right) \left( \frac{1}{57.3} \right) - p_C \left( \frac{5}{5+s} \right) \left( \frac{s+2}{s} \right) \right] (.365) \quad (C-17)$$

$$\text{Roll Mech Input} = F_{AS} (.24)(10) \left( \frac{1}{57.3} \right) \left( \frac{.3}{2} \right) \quad (C-18)$$

Recalling that:

$$\text{Roll Mech Input} + \text{Roll Elec Input} = 2 \delta_{DT} \quad (C-19)$$

$$F_{AS} \left( \frac{.0019s^2 + .0127s + .0128}{s + .3s^2} \right) - p \left( \frac{.365s + .73}{s} \right) + p_c \left( \frac{1.825s + 3.65}{5s + s^2} \right) = 2 \delta_{DT} \quad (C-20)$$

The augmented yaw axis flight control equation can be obtained from Fig. 20.

$$F_{RP} \left( \frac{.0087s + .174}{s + 10} \right) = \beta \left( \frac{1.035s + .5182}{s} \right) + \alpha P_o \left( \frac{.78s + .39}{s + 1} \right) +$$

$$p \left( \frac{(.78\alpha_o - .0039)s^2 + (.39\alpha_o - .0058)s - .0019}{s^2 + s} \right) +$$

$$r \left( \frac{(.14\alpha_o - 3.41)s^3 + (.21\alpha_o - 1.755)s^2 + (.105\alpha_o - .0376)s + (.0175\alpha_o - .0063)}{4s^3 + 4s^2 + s} \right)$$

$$+ \delta_{DT} \left( \frac{.103s + .0517}{s} \right) + \delta_R \left( \frac{.776s - .0789}{s} \right) \quad (C-21)$$

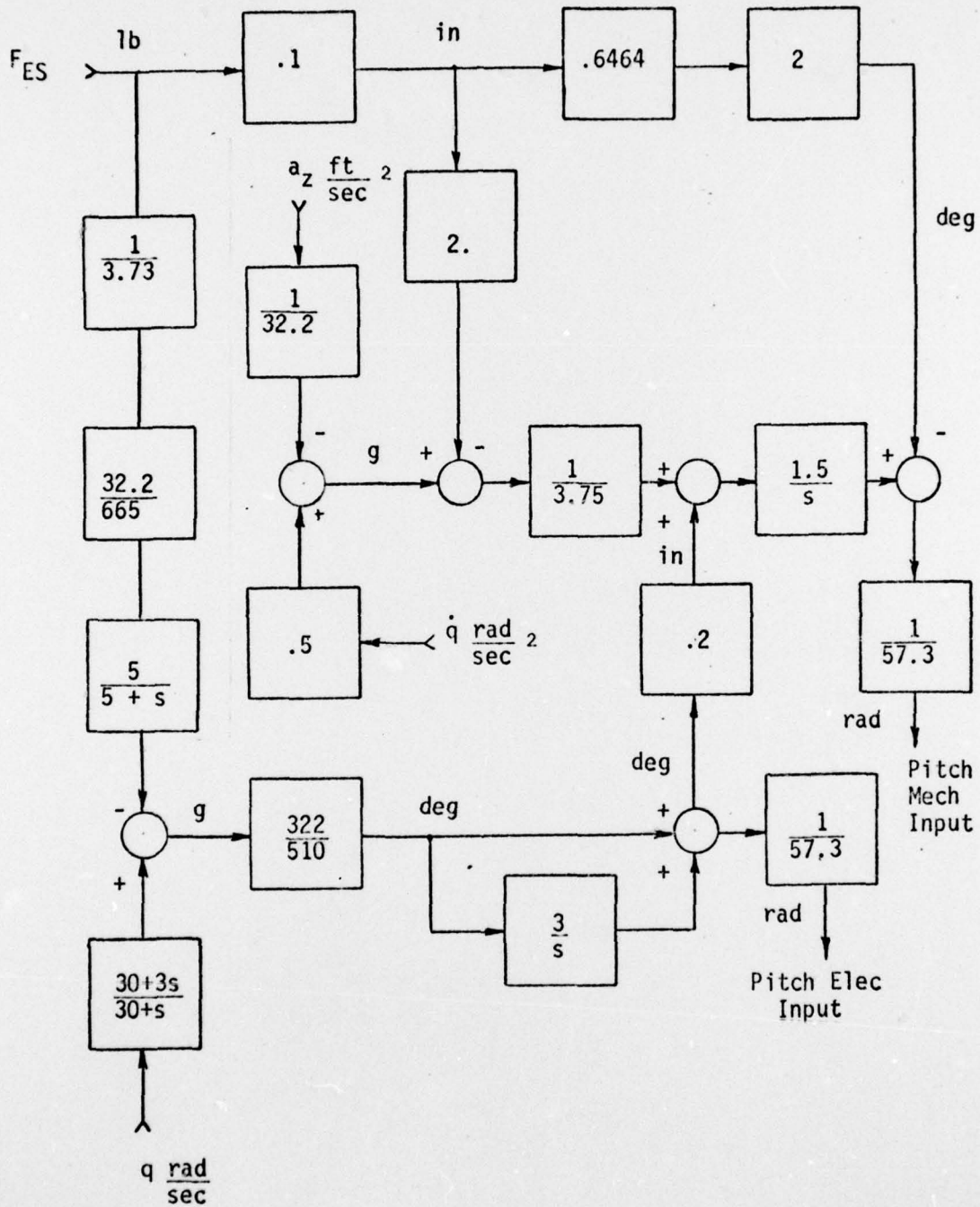


Fig. 18. Augmented Pitch Axis Control Laws (Firefly)

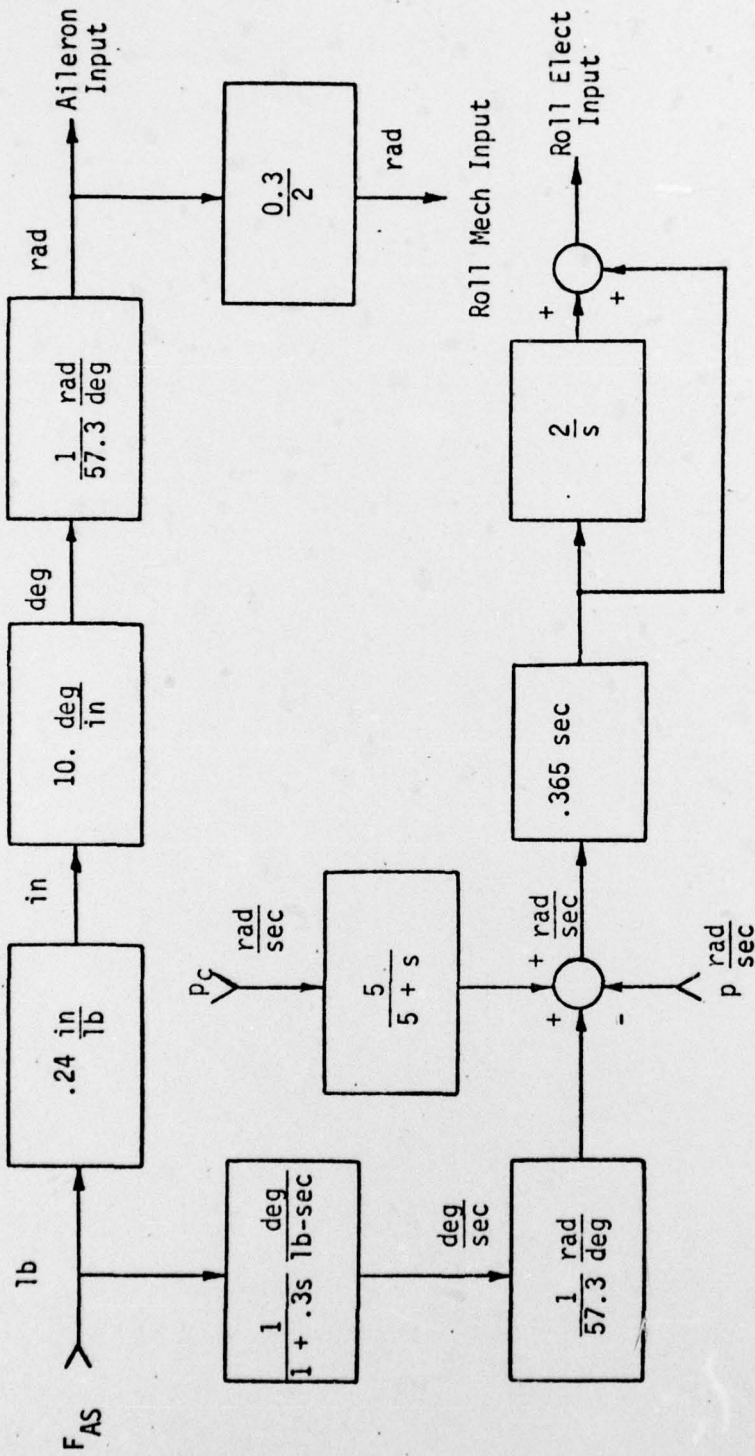


Fig. 19. Augmented Roll Axis Control Laws (Firefly)

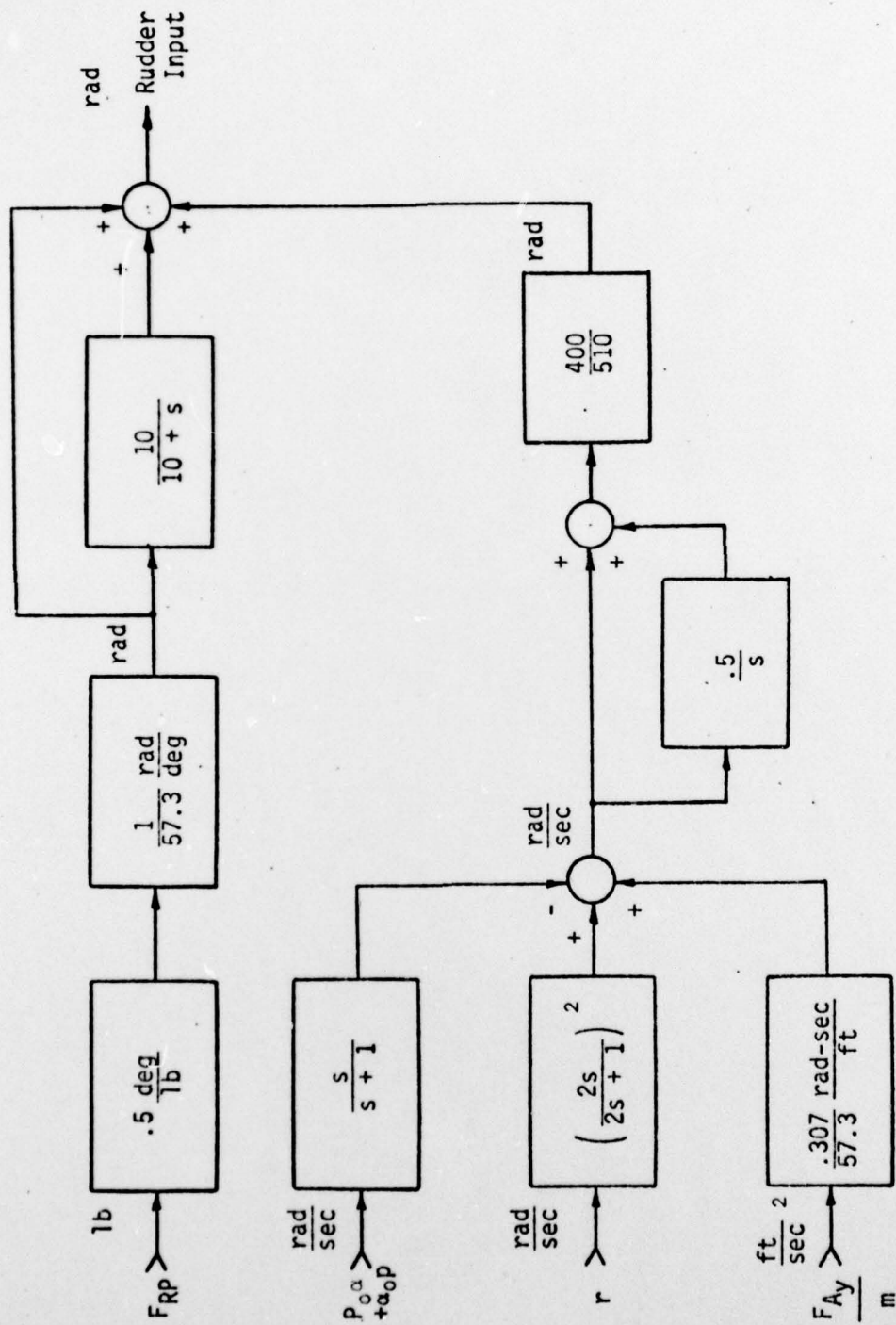


Fig. 20. Augmented Yaw Axis Control Laws (Firefly)

## Appendix D

### Computer Model

The computer program "FRQRSP" is a general purpose frequency response program which can be used to evaluate a system model and plot amplitude and phase response of a linear transfer function over a specified frequency range. It is also capable of solving a set of simultaneous equations by the Gauss Jordan elimination method (Ref 12:17). Additionally, the program is set up to perform spectrum analysis. The evaluation of the system is accomplished by first defining a function  $G(s)$  where  $s$  is the Laplace transform variable. The transfer functions in this report have been defined as:

1. The open loop response of the system ( $\phi$  and  $\phi_C$ ) to a lateral stick input.
2. The open loop response of the system ( $\phi$  and  $\phi_C$ ) to wind gust inputs.
3. The closed loop response of the system ( $\phi$  and  $\phi_C$ ) to wind gust inputs (pilot in the loop).
4. The closed loop response of the system ( $\phi_C$ ) to wind gust inputs (automatic fire control system).

In order to model the system for the computer program, it is necessary to set up the following complex matrix equation:

$$[A][R] = [B]$$

where  $[A]$  - Represents the system components which consist of the aircraft, the flight controls, and the fire control law (Figure 21 provides a listing of the matrix elements while figure 22 depicts the position of the non zero elements in the matrix).

- $[R]$  - The unknown vector representing the system variables.  
 -  $[u \ \beta \ \alpha \ p \ q \ r \ \psi \ \theta \ \phi \ \delta_{HT} \ \delta_A \ \delta_{DT} \ \delta_R \ t_f \ \lambda \ c_{p_w} \ d_{TN} \ \omega_w \ r_{Dz} \ p_c]^T$
- $[B]$  - The vector which represents the external inputs to the system such as wind gusts and lateral stick inputs (see figures 23 and 24 ).

The abbreviations used to define the A and B matrices in the computer program (Fig. 21 , 23 and 24 ) are listed below in terms of the symbols used in this report.

Fixed inputs:

$$ALAM\emptyset = \lambda_o$$

$$DK = K_D$$

$$E = b$$

$$GC = g_c$$

$$H = h$$

$$K\emptyset = K$$

$$PI = \pi$$

$$RHO = \rho/\rho_o$$

$$RT\emptyset = R_{T_o}$$

$$TF\emptyset = T_{f_o}$$

$$VT\emptyset = V_{T_o}$$

Ranges :

$$G\emptyset = G_o$$

$$RP\emptyset = R_{p_o}$$

$$RR\emptyset = R_{R_o}$$

$$RTV = R_{T_v}$$

$$R2 = R_2$$

Velocities:

$$U\emptyset = U_o$$

$$V\emptyset = V_o$$

$$W\emptyset = W_o$$

$$P\emptyset = P_o$$

$$Q\emptyset = Q_o$$

$$R\emptyset = R_o$$

Bombing Law Components:

$$CPW\emptyset = C_{P_{W_o}}$$

$$DTN\emptyset = D_{TN_o}$$

$$PC\emptyset = P_{C_o}$$

$$RDZ\emptyset = R_{DZ_o}$$

$$WOMEGA\emptyset = \omega_{W_o}$$

Angles:

$$A\emptyset = \alpha_o$$

$$B\emptyset = \beta_o$$

$$G\emptyset = \gamma_o$$

$$F\emptyset = \phi_o$$

$$S\emptyset = \psi_o$$

$$T\emptyset = \theta_o$$

Trigonometric functions:

$$SA\emptyset = \sin\alpha_o$$

$$SB\emptyset = \sin\beta_o$$

$$SF\emptyset = \sin\phi_o$$

$$SG\emptyset = \sin\gamma_o$$

$$SL\emptyset = \sin\lambda_o$$

$$SS\emptyset = \sin\psi_o$$

$$ST\emptyset = \sin\theta_o$$

$$CA\emptyset = \cos\alpha_o$$

$$CB\emptyset = \cos\beta_o$$

$$CF\emptyset = \cos\phi_o$$

$$CG\emptyset = \cos\gamma_o$$

$$CL\emptyset = \cos\lambda_o$$

$$CS\emptyset = \cos\psi_o$$

$$CT\emptyset = \cos\theta_o$$

To determine the system variables in  $[R]$ , the A matrix must be inverted. This procedure uses pivoting in order to maintain an accurate solution. Note that the ICOL statements following each element place

the element in the correct column for that row.

The parameter  $P(i)$  is used to correlate the inputs with the correct data. For this program, the P parameters are defined as:

P(1) - Pilot gain.

P(2) - Longitudinal input (not used).

P(3) - Lateral input.

P(4) - Horizontal wind gust input.

P(5) - Vertical wind gust input.

P(6) - P wind gust input.

P(7) - System gain.

To obtain the frequency response, the user supplied complex function  $G(s)$  is evaluated for a region of frequencies defined by the input data. The frequency is reported in both radians per second and hertz in tabular form, however, the Bode plots are in hertz. The amplitude of  $G(s)$  is reported as magnitude and decibels where decibels are defined to be  $20 \log_{10} |G(s)|$ . The phase of  $G(s)$  is reported in degrees as the arctangent of the imaginary part divided by the real part (Ref 12 :4).

For the PSD analysis, the user must again supply the complex transfer function  $G(s)$  where the input PSD is a real function in terms of radians per second or  $\omega$ . The results of the PSD analysis consists of a tabulation of the input and output PSD in both magnitude and decibels where the dB values are defined as  $10 \log_{10} |\text{PSD}|$ . The program also tabulates and plots the cumulative input and output power which is the square root of the input and output PSD magnitude values integrated from the starting frequency to the current frequency. When the program completes the evaluation of the input and output PSD values

over the specified range, the final cumulative power values are reported as the root mean square (RMS) values (Ref 12:5).

# BEST AVAILABLE COPY

```

DEFINE A IN FULL MATRIX FORM

DIMENSION A(20,20)
COMPLEX A,S
S IS THE LAPLACE TRANSFORM VARIABLE

A(1,1)=0.86*(3.782*A0*SA0-.020*CA0+.0905*A0*CA0-2.325*A0**2*CA0)-S
$ ICOL(1,1)=1
A(1,2)=565.*P0 $ ICOL(1,2)=2
A(1,3)=286.*(3.802*SA0-.868*A0*CA0+.0905*CA0-.0905*A0*SA0+2.325*
CA0**2*SA0)-665.*Q0 $ ICOL(1,3)=3
A(1,4)=-W0 $ ICOL(1,4)=5
A(1,5)=-32.2*CT0 $ ICOL(1,5)=8

A(2,1)=-R0 $ ICOL(2,1)=1
A(2,2)=-(.245.3+565.*S) $ ICOL(2,2)=2
A(2,3)=565.*P0 $ ICOL(2,3)=3
A(2,4)=W0+.918 $ ICOL(2,4)=4
A(2,5)=2.945-3.294*A0-U0 $ ICOL(2,5)=6
A(2,6)=-32.2*ST0*SFO $ ICOL(2,6)=8
A(2,7)=32.2*CT0*CF0 $ ICOL(2,7)=9
A(2,8)=-24.6 $ ICOL(2,8)=12
A(2,9)=37.52 $ ICOL(2,9)=13

A(3,1)=Q0+.86*(-3.782*A0*CA0-.020*SA0+.0905*A0*SA0-2.325*A0**2*SA0.
C) $ ICOL(3,1)=1
A(3,2)=-665.*P0 $ ICOL(3,2)=2
A(3,3)=286.*(-3.802*CA0-.868*A0*SA0+.0905*A0*CA0+.0905*SA0-2.325*
CA0**2*CA0)-665.*S $ ICOL(3,3)=3
A(3,4)=U0 $ ICOL(3,4)=5
A(3,5)=-32.2*ST0*CF0 $ ICOL(3,5)=8
A(3,6)=-32.2*CT0*SFO $ ICOL(3,6)=9

A(4,1)=-1.23-7.735*A0 $ ICOL(4,1)=2
A(4,2)=-.102-.0253*S-.0008*Q0 $ ICOL(4,2)=4
A(4,3)=-.0008*P0-.0197*F0 $ ICOL(4,3)=5
A(4,4)=.0204+2.833*A0-.0008*S-.0197*Q0 $ ICOL(4,4)=5
A(4,5)=.494 $ ICOL(4,5)=11
A(4,6)=.5556 $ ICOL(4,6)=12
A(4,7)=.0433-.116*A0 $ ICOL(4,7)=13

A(5,1)=-1.47-.0717*S $ ICOL(5,1)=3
A(5,2)=.0015*P0+.150*R0 $ ICOL(5,2)=4
A(5,3)=-.221-.1557*S $ ICOL(5,3)=5
A(5,4)=.150*P0-.0016*F0 $ ICOL(5,4)=6
A(5,5)=-3.416 $ ICOL(5,5)=10

A(6,1)=2.43-6.187*A0 $ ICOL(6,1)=2
A(6,2)=-.01275-.0008*S-.130*Q0 $ ICOL(6,2)=4
A(6,3)=-.130*P0+.0009*R0 $ ICOL(6,3)=5
A(6,4)=-.1263-.1755*S+.0009*Q0 $ ICOL(6,4)=6
A(6,5)=.0607-.551*A0 $ ICOL(6,5)=11
A(6,6)=.303 $ ICOL(6,6)=12
A(6,7)=-1.14 $ ICOL(6,7)=13

```

Fig. 21. Elements of the A Matrix

# BEST AVAILABLE COPY

```

A(7,1)=SF0/CT0      $ ICOL(7,1)=5
A(7,2)=CF0/CT0      $ ICOL(7,2)=6
A(7,3)=-S           $ ICOL(7,3)=7
A(7,4)=(TAN(T0)/CT0)*(OC*SF0+R0*CF0)  $ ICOL(7,4)=8
A(7,5)=R0*CF0/CT0-R0*SF0/CT0      $ ICOL(7,5)=9

A(8,1)=CF0          $ ICOL(8,1)=5
A(8,2)=-SF0         $ ICOL(8,2)=6
A(8,3)=-S           $ ICOL(8,3)=8
A(8,4)=-R0*SF0+R0*CF0  $ ICOL(8,4)=9

A(9,1)=1.           $ ICOL(9,1)=4
A(9,2)=SF0*TAN(T0)  $ ICOL(9,2)=5
A(9,3)=CF0*TAN(T0)  $ ICOL(9,3)=6
A(9,4)=R0*SF0/CT0+R0*CF0/CT0*2  $ ICOL(9,4)=8
A(9,5)=R0*CF0*TAN(T0)-R0*SF0*TAN(T0)-S  $ ICOL(9,5)=9

A(10,1)=.0267*(-3.782*AO*CAJ-.020*SA0+.0905*AO*SAJ-2.325*AO**2*
CSAJ)*(0.0785*S**3+.8816*S**2+.835*S+.2356)/(S**3+30.*S**2)
C $ ICOL(10,1)=1
A(10,2)=.8387*(-3.8J2*CA0-.863*AO*SAJ+.0905*AO*CAJ+.0905*SA0-
02.325*AO**2*CAJ)*(0.0786*S**3+.8816*S**2+.835*S+.2356)/(S**3+30.*
CS**2) $ ICOL(10,2)=3
A(10,3)=(.1603*S**4+4.798*S**3+36.14*S**2+40.24*S+3.94)/(3.*S**3+
091.*S**2+30.*S) $ ICOL(10,3)=5
A(10,4)=-1.         $ ICOL(10,4)=10

A(11,1)=23.87       $ ICOL(11,1)=11
A(11,2)=(1./S)*(P(1)*(0.5*S+1.)*CEXP(-.3*S))  $ ICOL(11,2)=20

A(12,1)=.0625       $ ICOL(12,1)=4
A(12,2)=2.          $ ICOL(12,2)=12
A(12,3)=(1./S)*P(1)*(0.5*S+1.)*CEXP(-.3*S)*((.0019*S+.0074)/(3.*
CS+1.))  $ ICOL(12,3)=20

A(13,1)=(1.103*S+.555)/S  $ ICOL(13,1)=2
A(13,2)=(.34*PJ*S+.42*P(1))/(S+1.)  $ ICOL(13,2)=3
A(13,3)=((.84*AO-.0041)-S**2+(.42*AO-.0062)*S-.0021)/(S**2+S)
C $ ICOL(13,3)=4
A(13,4)=((.1436*AO-3.413)*S**3+1.224J*AO-1.76)*S**2+(.1122*AO-
C.1397)*S+.0187*AO-.0066)/(4.*S**3+4.*S**2+S)  $ ICOL(13,4)=5
A(13,5)=(.1107*S+.0553)/S  $ ICOL(13,5)=12
A(13,6)=(.8307*S-.0845)/S  $ ICOL(13,6)=13

A(14,1)=-ST0  $ ICOL(14,1)=1
A(14,2)=VT0*CT0*SF0  $ ICOL(14,2)=2
A(14,3)=W0*CT0*CF0  $ ICOL(14,3)=3
A(14,4)=-U0*CT0-W0*ST0*CF0  $ ICOL(14,4)=8
A(14,5)=-R0*CT0*SF0  $ ICOL(14,5)=9
A(14,6)=-U0*ST0+VT0*SA0*CT0*CF0+GC*TF0/TF0  $ ICOL(14,6)=14

```

Fig. 21. (Continued) Elements of the A Matrix

# BEST AVAILABLE COPY

```

A(15,1)=CA0*(-.5*ST0*OK*RHO*TF0**3*GC)+SA0*(.5*CT0*CF0*OK*RHO*
CTF)**3*GC) § ICOL(15,1)=1
A(15,2)=CB0*((CS0*ST0*ST0*SS0*CF0)*PT0*CG0+CT0*SF0*RT0*SG0-.5*
CG0*SF0*DP*GC*TF0**2) § ICOL(15,2)=2
A(15,3)=-SA0*(CS0*CT0*RT0*CG0-ST0*RT0*SF0+.5*ST0*DP*GC*TF0**2)+
CC0*((CS0*ST0*CF0)+SS0*SF0)*RT0*CG0+CT0*CF0*RT0*SG0-.5*CT0*CF0*DP*
CG0*TF0**2) § ICOL(15,3)=3
A(15,4)=CA0*(-SS0*CT0*PT0*CG0)+SA0*((-SS0*ST0*CF0+CS0*SF0)*RT0*
CG0) § ICOL(15,4)=7
A(15,5)=CA0*(-CS0*ST0*RT0*CG0-CT0*RT0*SG0+.5*CT0*DP*GC*TF0**2)+
CS0*(CS0*CT0*CF0*RT0*CG0-ST0*CF0*RT0*SG0+.5*ST0*CF0*DP*GC*TF0**2)
ICOL(15,5)=9
A(15,6)=SA0*((-CS0*ST0*SF0+SS0*CF0)*RT0*CG0-CT0*SF0)*RT0*SG0+.5*
CG0*SF0*DP*GC*TF0**2) § ICOL(15,6)=9
A(15,7)=(CA0*ST0-SA0*CT0*CF0)*(DP*GC*TF0-.5*OK*RHO*SC*VT0*TF0**2)
ICOL(15,7)=14
A(15,8)=RPO*SL0 § ICOL(15,8)=15

A(16,1)=(-.5*OK*RHO*TF0**3*GC)*CA0*CT0*SF0 § ICOL(16,1)=1
A(16,2)=-SA0*(RT0*CG0*(CS0*ST0)*SF0-SS0*CF0)+RT0*SG0*CT0*SF0-.5*DP*
CG0*TF0**2*CT0*SF0) § ICOL(16,2)=3
A(16,3)=-CA0*(RT0*CG0*(SS0*ST0*SF0+CS0*CF0)) § ICOL(16,3)=7
A(16,4)=CA0*(RT0*CG0*(CS0*CT0*SF0)-RT0*SG0*ST0*SF0+.5*DP*GC*TF0**2
*ST0*SF0) § ICOL(16,4)=8
A(16,5)=CA0*(RT0*CG0*(CS0*ST0*CF0+SS0*SF0)+RT0*SG0*CT0*CF0-.5*DP*
CG0*TF0**2*CT0*CF0) § ICOL(16,5)=9
A(16,6)=CA0*(-DP*GC*TF0*CT0*SF0+.5*OK*RHO*VT0*GC*TF0**2*CT0*SF0)
ICOL(16,6)=14
A(16,7)=-1. § ICOL(16,7)=16

A(17,1)=-RPO**2/(2.*VT0**2)-DP**2*TF0**2/2.+VT0*TF0**2*DP*OK*RHO*
CTF) § ICOL(17,1)=1
A(17,2)=-DP**2*VT0*TF0+VT0*TF0**2*DP*OK*RHO*VT0 § ICOL(17,2)=14
A(17,3)=-1. § ICOL(17,3)=17

A(18,1)=-CA0*286.*.8595/VT0 § ICOL(18,1)=2
A(18,2)=CA0*286.*.90321/VT0 § ICOL(18,2)=4
A(18,3)=CA0*286.*(.0103-.020*AG)/VT0 § ICOL(18,3)=6
A(18,4)=CA0*(-GC*ST0*SF0)/VT0 § ICOL(18,4)=5
A(18,5)=CA0*(GC*CT0*CF0)/VT0 § ICOL(18,5)=9
A(18,6)=CA0*286.*(-.086)/VT0 § ICOL(18,6)=12
A(18,7)=CA0*286.*.1312/VT0 § ICOL(18,7)=13
A(18,8)=-1. § ICOL(18,8)=13

A(19,1)=RPO*CL0 § ICOL(19,1)=15
A(19,2)=-1. § ICOL(19,2)=19

A(20,1)=K0/RD20 § ICOL(20,1)=16
A(20,2)=-K0*WOMEGA0/RD20 § ICOL(20,2)=17
A(20,3)=-K0*DTN0/RD20 § ICOL(20,3)=18
A(20,4)=-K0*(CPWJ-DTNC*WOMEGA0)/RD20**2 § ICOL(20,4)=19
A(20,5)=-1. § ICOL(20,5)=20

```

Fig. 21. (Continued) Elements of the A Matrix



# BEST AVAILABLE COPY

```

R(1)=-((286.*(3.80*SA0-.868*A0*CA0+.0905*CA0-.0905*A0*SA0+2.325*A0
C**2*SA0)/VT0)*P(5)
R(2)=((+245.8)/VT0-(2.946-8.294*A0)*((-S/VT0)/(1.+(3.*E*S)/(PI*
CVT0))))*P(4)-.918*P(6)
R(3)=-((286.*(-3.80*CA0-.868*A0*SA0+.0905*A0*CA0+.0905*SA0-2.325*
CA0**2*CA0)/VT0)*P(5)
R(4)=((+1.29+3.335*A0)/VT0-(.0204+2.833*A0)*((-S/VT0)/(1.+(3.*E
C*S)/(PI*VT0))))*P(4)+.102*P(6)
R(5)=((+1.47)/VT0-(-.221+.0717)*(S/VT0)/(1.+(4.*E*S)/(PI*VT0
C))))*P(5)
R(5)=-((2.43-6.19*A0)/VT0-(-.1063)*((-S/VT0)/(1.+(3.*E*S)/(PI*
CVT0))))*P(4)+.01276*P(6)
R(10)=(.0023*S**3+.044*S**2+.0526*S+.0105)/(S**3+5.*S**2)*P(2)
C+((-8.885*(-3.802*CA0-.868*A0*SA0+.0905*A0*CA0+.0905*SA0-2.325*A0
C**2*CA0)*(+.0786*S**3+.8916*S**2+.835*S+.2756)/(S**3+30.*S**2))
C/VT0)*P(5)
R(11)=1.*P(3)
R(12)=(.0019*S+.0074)/(.3*S+1.)*P(3)
R(13)=(((-(1.11*S+.555)/S)/VT0)*((.013-.037*A0)*S+(.007-.019*A0))
C/S)*((-S/VT0)/(1.+(3.*E*S)/(PI*VT0))))*P(4)+((.004*S+.002)/S)*P(6)

```

Fig. 23. Elements of the B Matrix (Basic F-15)

```

R(1)=-((286.*(3.80*SA0-.868*A0*CA0+.0905*CA0-.0905*A0*SA0+2.325*A0
C**2*SA0)/VT0)*P(5)
R(2)=((+245.8)/VT0-(2.946-8.294*A0)*((-S/VT0)/(1.+(3.*E*S)/(PI*
CVT0))))*P(4)-.918*P(6)
R(3)=-((286.*(-3.80*CA0-.868*A0*SA0+.0905*A0*CA0+.0905*SA0-2.325*
CA0**2*CA0)/VT0)*P(5)
R(4)=((+1.29+3.335*A0)/VT0-(.0204+2.833*A0)*((-S/VT0)/(1.+(3.*E
C*S)/(PI*VT0))))*P(4)+.102*P(6)
R(5)=((+1.47)/VT0-(-.221+.0717)*(S/VT0)/(1.+(4.*E*S)/(PI*VT0
C))))*P(5)
R(5)=-((2.43-6.19*A0)/VT0-(-.1063)*((-S/VT0)/(1.+(3.*E*S)/(PI*
CVT0))))*P(4)+.01276*P(6)
R(10)=((-8.885*(-3.802*CA0-.868*A0*SA0+.0905*A0*CA0+.0905*SA0
C-2.325*A0**2*CA0)*(+.0786*S**2+.049*S+.2356)/(30.*S**2+S**3))/VT0
C)*P(5)
R(11)=1.*P(3)
R(12)=(.0019*S+.0074)/(.3*S+1.)*P(3)
R(13)=(((-(1.03*S+.52)/S)/VT0)*((.012-.035*A0)*S+(.006-.017*A0))/S
C)*((-S/VT0)/(1.+(3.*E*S)/(PI*VT0))))*P(4)+((.0039*S+.0019)/S)*P(6)

```

Fig. 24. Elements of the B Matrix (Automatic Fire Control System)

### Vita

Joel Dana Walton was born in Dillon, Montana in September, 1944. He enlisted in the U.S. Air Force in 1965 and spent one year as an air traffic controller prior to attending college at the University of Arizona through the Airman's Education and Commissioning Program. He graduated with a B.S. degree in Aeronautical Engineering in January 1969 and then attended Officers Training School (OTS). Upon graduation from OTS he entered Undergraduate Pilot Training at Williams AFB, Arizona, and graduated in June, 1970. After attending the Forward Air Controller (FAC) course at Eglin AFB, Florida, he was reassigned to Pleiku AB, Vietnam, as a FAC in the O-2A aircraft. Upon his return to the states in November, 1971, he was assigned to Fairchild AFB, Washington, as a pilot in the B-52 aircraft. He spent a four year tour as a pilot and instructor pilot prior to entering the Air Force Institute of Technology in June, 1976.

Permanent address: Box 123  
Dawson Creek, B.C., Canada

UNCLASSIFIED

SECURITY CLASSIFICATION OF THIS PAGE (When Data Entered)

14 REPORT DOCUMENTATION PAGE		READ INSTRUCTIONS BEFORE COMPLETING FORM
1. REPORT NUMBER AFIT/GAE/AA/77D-17	2. GOVT ACCESSION NO.	3. DEPARTMENT CATALOG NUMBER
4. TITLE (and Subtitle) A FEASIBILITY STUDY OF A MANUAL BOMB RELEASE WHILE IN A TURN.		5. TYPE OF REPORT, PERIOD COVERED MS Thesis
7. AUTHOR 10 Joel D. Walton Capt. USAF		6. PERFORMING ORG. REPORT NUMBER
9. PERFORMING ORGANIZATION NAME AND ADDRESS Air Force Institute of Technology (AFIT-EN) Wright-Patterson AFB, Ohio 45433		8. CONTRACT OR GRANT NUMBER(s)
11. CONTROLLING OFFICE NAME AND ADDRESS Air Force Avionics Laboratory RWT Wright-Patterson AFB, Ohio 45433		10. PROGRAM ELEMENT, PROJECT, TASK AREA & WORK UNIT NUMBERS 16 1987-164 17 01
14. MONITORING AGENCY NAME & ADDRESS (if different from Controlling Office)		12. REPORT DATE 11 December 1977
		13. NUMBER OF PAGES 12 123p
		15. SECURITY CLASS. (of this report) Unclassified
16. DISTRIBUTION STATEMENT (of this Report) Approved for public release; distribution unlimited.		15a. DECLASSIFICATION/DOWNGRADING SCHEDULE
17. DISTRIBUTION STATEMENT (of the abstract entered in Block 20, if different from Report)		
18. SUPPLEMENTARY NOTES Approved for public release; IAW AFR 190-17 JERAL F. GUESS, Captain, USAF Director of Information		
19. KEY WORDS (Continue on reverse side if necessary and identify by block number) Manual Bomb Run Closed Loop Tracking Performance Human Operator Theory		
20. ABSTRACT (Continue on reverse side if necessary and identify by block number) ➤ This study attempts to determine if a pilot can manually release a bomb while in a turn. The nonlinear equations describing the geometry, fire control law, aircraft equations of motion, flight controls and pilot model are developed. These equations are linearized so that a frequency response analysis can be conducted for perturbations about a nominal trajectory. The system response is evaluated using wind gust inputs and lateral stick inputs and plotting the resulting system perturbations over a given frequency range. ←		

012225